

**QUALITY MONITORING
OF RECYCLED PLASTIC WASTE
DURING EXTRUSION:
IN-LINE PARTICLE DETECTION**

by

Stella Desa

**A thesis submitted in conformity with the requirements
for the degree of Master of Applied Science
Graduate Department of Chemical Engineering and Applied Chemistry
University of Toronto**

© Stella Desa 1995



**National Library
of Canada**

**Acquisitions and
Bibliographic Services**

**395 Wellington Street
Ottawa ON K1A 0N4
Canada**

**Bibliothèque nationale
du Canada**

**Acquisitions et
services bibliographiques**

**395, rue Wellington
Ottawa ON K1A 0N4
Canada**

Your file Votre référence

Our file Notre référence

The author has granted a non-exclusive licence allowing the National Library of Canada to reproduce, loan, distribute or sell copies of this thesis in microform, paper or electronic formats.

The author retains ownership of the copyright in this thesis. Neither the thesis nor substantial extracts from it may be printed or otherwise reproduced without the author's permission.

L'auteur a accordé une licence non exclusive permettant à la Bibliothèque nationale du Canada de reproduire, prêter, distribuer ou vendre des copies de cette thèse sous la forme de microfiche/film, de reproduction sur papier ou sur format électronique.

L'auteur conserve la propriété du droit d'auteur qui protège cette thèse. Ni la thèse ni des extraits substantiels de celle-ci ne doivent être imprimés ou autrement reproduits sans son autorisation.

0-612-45466-5

Canada

QUALITY MONITORING OF RECYCLED PLASTIC WASTE DURING EXTRUSION: IN-LINE PARTICLE DETECTION

**Master of Applied Science
1995**

Stella Desa

**Graduate Department of Chemical Engineering and Applied Chemistry
University of Toronto**

ABSTRACT

An In-Line Particulate Vision Monitor was developed to optically detect and quantify particulate contaminants present in recycled plastic waste during extrusion. The monitor, equipped with fibre optic probes, is capable of detecting particles in the range of 10 to 1 000 μm . Four batches of recycled polyethylene were evaluated at 200°C and 30 rpm. All batches possessed bimodal particle area distributions with projected particle areas ranging from 30 to 25 000 μm^2 .

The performance of the monitor was further assessed by studying melt filtration in-line, through both transient and pulse response testing techniques. An increase in the extrusion temperature resulted in an increase of the number of fine particles passing through the Dutch weave filter. The present quality monitor could be integrated into a process control scheme in order to manipulate the concentration and distribution of particulate contaminants in recycled plastic waste.

ACKNOWLEDGEMENTS

In the course of pursuing this thesis there were many individuals who aided my efforts. In particular I would like to thank my supervisor, Professor Balke, for providing valuable guidance and encouragement. I would also like to express thanks to my other supervisor, Professor Cluett, for his support.

I appreciate the technical assistance provided by Nikolay Stoev at the Ontario Laser and Lightwave Research Centre. The contributions received from High-Technology Corporation and Resource Plastics Corporation are gratefully acknowledged. I wish to thank the Ontario Centre for Materials Research and the Natural Sciences and Engineering Research Council of Canada for providing the funding needed to accomplish this work.

Special thanks are due to my fellow graduate students, Mark Tempel, Ramin Reshadat, Ronnie Salerni, Shang Hsu, and Paul Cheung, for their most generous help in day to day activities.

Finally, I would like to thank my family for their love, support and understanding.

TABLE OF CONTENTS

Abstract	ii
Acknowledgements	iii
Table of Contents	iv
List of Figures	vi
List of Tables	vii
1.0 INTRODUCTION	1
2.0 LITERATURE SURVEY AND THEORY	4
2.1 Plastics Recycling	4
2.2 In-line and On-line Monitoring of Polymer Processing via Fibre Optics	6
2.2.1 Principles of Fibre Optics: Optical Fibres	6
2.2.2 Fibre Optic Assisted Spectrophotometry in Monitoring Polymer Processes	8
2.2.3 Particle Imaging for Monitoring Polymer Processing	10
2.3 Melt Filtration	11
2.4 Residence Time Distribution	14
3.0 DEVELOPMENT OF THE IN-LINE PARTICULATE VISION MONITOR	18
3.1 Interface Design	19
3.1.1 Five-window Cylindrical Interface	19
3.1.2 Die Strand Interface	23
3.2 Image Formation and Analysis	26
3.2.1 Image processing and analysis	27
3.3 Novelty of the In-Line Particulate Vision Monitor Design	28
4.0 EXPERIMENTAL PROCEDURES	30
4.1 Utility Assessment of the Particulate Vision Monitor	30
4.2 Assessment of Melt Filtration	32
4.2.1 Transient Testing	33
4.2.2 Pulse Response Testing	34
5.0 RESULTS AND DISCUSSION	36
5.1 Utility Assessment of the Particulate Vision Monitor	36

5.1.1	Image Interpretation	36
5.1.2	Evaluation of Recycled Polyethylene	47
5.2	Assessment of Melt Filtration	53
5.2.1	Transient Testing	53
5.2.2	Pulse Response Testing	56
5.2.2.1	Glass Bead Size Distribution	56
5.2.2.2	Residence Time Distribution	56
6.0	CONCLUSIONS	61
7.0	RECOMMENDATIONS	63
8.0	REFERENCES	65
	APPENDIX A: Equipment Specifications for Illumination, Detection and Image Analysis System	68
	APPENDIX B: Histograms of Recycled Polyethylene and Blank Image Guide	70
	APPENDIX C: Particle Area Distribution: Sample Calculation	71
	APPENDIX D: In-Line and Off-Line Images of Recycled High Density Polyethylene	72
	APPENDIX E: Particle Concentration: Sample Calculation	75
	APPENDIX F: Residence Time Distribution: Sample Calculation	76

LIST OF FIGURES

Figure 1	Schematic of an Optical Fibre	7
Figure 2	Acceptance Cone of an Optical Fibre	7
Figure 3	Slide-Plate Screen Changer	12
Figure 4	Pressure Profile for a Typical Discontinuous and Continuous Melt Filtration System	13
Figure 5	Continuous Screen Changer	14
Figure 6	Overview of In-Line Particulate Vision Monitor	18
Figure 7	Five-Window Cylindrical Interface	20
Figure 8	Die Strand Interface: centre cross-section and front view	24
Figure 9	Die Strand Interface: side, top and bottom view	25
Figure 10	In-Line Particulate Vision Monitor	26
Figure 11	In-Line Evaluation of Recycled Polyethylene	30
Figure 12	In-Line Evaluation of Melt Filtration	32
Figure 13	In-Line Image of Recycled Polyethylene (A-HDPE) During Extrusion (200°C, 30 rpm)	37
Figure 14	Interpretation Algorithm for In-Line Images	37
Figure 15	Median Filtered Image (median filter applied 5 times)	39
Figure 16	Histogram Minimum Method: Selected Area	39
Figure 17	Grey Level Histogram of Selected Area on Figure 16	41
Figure 18	250 μm Diameter Glass Beads	41
Figure 19	Processed Image of Figure 15	43
Figure 20	Particle Area Distribution of Particulate Contaminants in	

	Recycled High Density Polyethylene (A-HDPE) Based on 1 Image	43
Figure 21	Effect of Accumulating Images on the Particle Area Distribution	45
Figure 22	Height of Particle Area Distribution versus Number of Images Used (material= A-HDPE)	46
Figure 23	Particle Area Distribution of A-HDPE, 10 images	48
Figure 24	Particle Area Distribution of B-HDPE, 10 images	48
Figure 25	Particle Area Distribution of C-HDPE, 10 images	49
Figure 26	Particle Area Distribution of D-LDPE, 10 images	49
Figure 27	Off-Line Image of D-LDPE (200°C, transmission illumination)	51
Figure 28	In-Line Image of D-LDPE During Extrusion (200°C, 30 rpm)	51
Figure 29	Pressure Difference Across Melt Filter versus Time	54
Figure 30	Interaction Plot: Effect of T and rpm on Glass Bead Distribution	57
Figure 31	Cumulative Time Distribution in a Single Screw Extruder	57

LIST OF TABLES

Table 2-1	Characterization Factors for Recycled Plastic Waste	5
Table 2-2	Applications of Fibre Optic Spectrophotometry in Monitoring Polymer Processes	8
Table 4-1	Recycled Polyethylene Evaluated In-Line	32
Table 4-2	Transient Testing of Melt Filtration	33
Table 4-3	Conditions for Pulse Response Testing	34
Table 4-4	Glass Bead Size Distribution	35
Table 5-1	Particulate Concentration in Recycled Polyethylene	53
Table 5-2	Melt Filtration: Effect of Temperature on Particle Removal	54
Table 5-3	Summary of Residence Time Distributions	58

1.0 INTRODUCTION

Particulate contaminants in recycled plastic waste can, depending upon their size and concentration, affect material processing and final product performance.^{1,2,3} Low contamination levels are critical for applications which require thin walls. In blow moulding, foreign materials will mar the appearance and degrade the properties of blow moulded parts. While in film production, particulates will introduce streaks and imperfections in the end product. Particulates typically consists of paper fibres, glass, metal, sand, geis, catalyst residuals or additive agglomerates. A portion of the contaminants present in recycled plastic waste may be removed through melt filtration. Because recycled plastic waste must compete with virgin resin, in-line quality monitoring of recycled plastic waste, for particle content, is of major importance.

In industry, particles are usually detected off-line. Thin films of polymer sample are subjected to back-lighting and defects are manually counted and classified into different size categories. Optical microscopy and light scattering techniques have also been used to determine the particle size distribution of particulates in molten polymer slabs.⁴ The disadvantages of off-line analysis include time delay, sparse sampling and the need for reprocessing to create film for inspection.

In-line monitoring of molten polymers has several advantages over off-line monitoring. In-line monitoring eliminates the need for handling hot, viscous molten polymers and the process analysis is conducted in a non-intrusive manner. Moreover, in-line monitoring reduces response time, reduces waste and results in a more uniform quality product.⁵

The use of fibre optic probes, owing to their ability to become an extension to either an illumination or a detection instrument, provides a viable means to overcome the high process temperatures and pressures encountered in monitoring a polymer process in-line.⁶ Furthermore, the wide availability of fibre optics and charged coupled device (CCD) detection systems serve to make the construction of an in-line video based particle monitor more attractive.

Currently there is only one commercially available instrument^{7,8,9} capable of imaging a variety of particles from 10 to 1 000 μm in polymer melts. This instrument, however, is not very satisfactory as it operates on-line, by monitoring a sample stream, as opposed to operating in-line. In addition, a published critical assessment of the images obtained, from this instrument, and their quantitative analysis is lacking.

The primary objective of this thesis is to develop an in-line particulate vision monitor which will operate in real time with an extruder to optically detect and quantify particulate contaminants present in recycled plastic waste. A key step in the development of the in-line monitor involves the design of a suitable interface. The interface enables sensitive fibre optic probes to interact with the high temperature and high pressure conditions that are typical of polymer flow inside an extruder.

The secondary objective is to assess the utility of the particulate vision monitor for monitoring the quality of recycled plastic waste in-line, as the material flows through an extruder. This will be accomplished through the in-line evaluation of four different grades of recycled polyethylene.

The third and final objective is to assess polymer melt filtration through the use of the in-line particle vision monitor. Melt filtration has not previously been studied in-line. The process of melt filtration will be evaluated through both transient and pulse response testing techniques. In transient testing, a filter cake is allowed to develop on the filter screen over a duration of six hours. In pulse response testing, a set quantity of glass beads is injected into the extruder. Pulse response testing yields information on the glass bead particles size distribution before and after the filter and is also used to determine the residence time distribution of the glass beads in the extrusion system.

2.0 LITERATURE SURVEY AND THEORY

2.1 PLASTICS RECYCLING

Recently, as public concern over the environmental problems associated with landfills has grown, increased attention has been focused on plastics recycling. Plastics represent only 7% by weight of the municipal waste stream but occupy 18% by volume of landfill space.¹⁰ Recycling offers a significant opportunity to reduce the amount of material in the solid waste stream and this movement is largely encouraged through government legislation.

Currently the U.S. plastics recycling rate is 4.5%, with half a billion kg/yr of polyethylene terephthalate (PET) and high density polyethylene (HDPE) bottles reclaimed. In Europe the plastics recycling rate stands at 7.5% with 1 billion kg/yr of plastics reclaimed.¹¹ The present trend indicates that the quantity of plastics being recycled is increasing at a rapid rate.

The main steps involved in the recycling of plastics are: collection of post consumer and process wastes, sorting of dissimilar materials, separation of labels and metallic components from the product, cleaning, washing of the plastic waste by water, detergents and solvents, drying, size reduction by granulation, compounding if necessary to provide ingredients in order to supplement those properties which have deteriorated as a result of already having been used once, extrusion, melt filtration and pelletizing.

The value of the recycled plastic is directly related to the purity of the material.¹² Even after sorting and washing, the waste polymer will likely contain polymeric, particulate and chemical contaminants.¹³ To ensure product adequacy, minimizing the following key

impurities¹⁴ is desired: particulate aluminum, paper, pigment colourants, glues and adhesives, other polymers and moisture. The following table¹⁴ is a summary of features which various suppliers consider to be important in characterizing recycled resin.

TABLE 2-1: Characterization Factors for Recycled Plastic Waste

<p>Molecular Weight Melt Index</p> <p>Composition Melting Point</p> <p>Physical Characteristics Density Bulk Density</p> <p>Other Odour Pesticide</p>	<p>Impurities Polyvinyl Chloride Chloride Aluminum Floaters Polypropylene Wood Paper Particle Size Sinkers PET Heavy metals Glue Ash</p>	<p>Properties Tensile strength Elongation Flexural Modulus Notched Izod</p>
---	---	--

Impurities may introduce problems during processing or in the final product. For instance, the amount of interpolymer contamination which can be tolerated depends on the end application, the degree and consequence of reaction between the dissimilar polymers, and processing stability of the polymer/polymer system. Metal contaminants, on the other hand, can plug the small channels found in processing equipment. The presence of metals in the final product can range from simply being considered aesthetically undesirable to reducing physical and other performance characteristics. In the end, the aim of any recycling program is to transform waste polymer into a value added product.

2.2 IN-LINE AND ON-LINE MONITORING OF POLYMER PROCESSING VIA FIBRE OPTICS

The availability of fibre optical devices and opto-electrical systems in recent years has prompted the growth of both in-line and on-line sensor technologies.¹⁵ In-line measurements are conducted in-situ by monitoring the process at an actual processing stream. On-line measurements, on the other hand, are performed on a side stream that has been diverted from the main processing line. On-line measurement technologies are used to control the quality of polymeric materials during all phases of production and for minimizing waste in the form of off-specification material. The most advanced developments in the process monitoring field involve fibre optic based devices which enable in-line monitoring of real systems under remote sensing conditions.

2.2.1 PRINCIPLES OF FIBRE OPTICS: OPTICAL FIBRES

Optical fibres allow the transmission of light over large distances. For monitoring a polymer process, 1 to 100 m is a realistic range. Optical fibres operate on the phenomenon of total internal reflection, as illustrated in Figure 1. Step index fibres consist of a core region of glass, having a refractive index, n_1 , surrounded by a cladding of lower refractive index, n_2 . Incident light will be transmitted through the fibre if it strikes the cladding at an angle greater than the critical angle, θ_c , so that it is totally internally reflected at the core/cladding interface.

The critical angle, θ_c , is defined as follows¹⁶:

$$\sin \theta_c = \frac{n_2}{n_1} \quad (2.1)$$

As shown in Figure 2, light entering the fibre within an acceptance cone is totally

reflected at the core/cladding interface, and will be transmitted through the fibre. The acceptance angle, α , depends on the refractive indices of the core and cladding, as well as on the refractive index of the surrounding medium, n_0 , (which is usually air)¹⁷:

$$\sin \alpha = \frac{(n_1^2 - n_2^2)^{1/2}}{n_0} \quad (2.2)$$

More commonly, the range of angles is described in terms of the numerical aperture (NA), defined as¹⁷:

$$NA = n_0 \cdot \sin \alpha \quad (2.3)$$

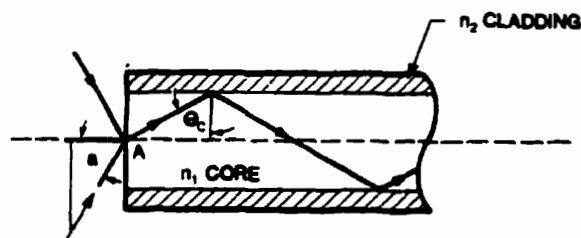


Figure 1: Schematic of an Optical Fibre

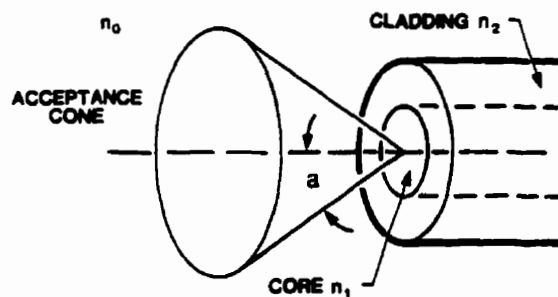


Figure 2: Acceptance Cone of an Optical Fibre

There are various types of optical fibre arrangements. Single fibres have high transmittance and preserve the brightness of the source; they are economic for covering large distances. Random or incoherent fibre bundles are composed of many close packed optical fibres and are used to transfer and collect light from sources and samples. Aligned or coherent fibres bundles consist of an ordered arrangement of fibres and are used to transfer light and images.

2.2.2 FIBRE OPTIC ASSISTED SPECTROPHOTOMETRY IN MONITORING POLYMER PROCESSES

During the past decade, on-line spectrophotometric analysis has become possible due to the prevalence of fibre optics.¹⁸ A fibre optic cable transmits light from a spectrophotometer to a probe which is interfaced to the polymer sample. The sample will characteristically absorb radiant energy. The remaining light is received by a second fibre optic probe and transmitted back to the spectrophotometer.

When the property of interest can be measured spectrophotometrically, fibre optics allow in-line and on-line measurements to be accomplished⁶. Table 2-2 lists some examples of features that have been measured using fibre optics.

TABLE 2-2: Applications of Fibre Optic Spectrophotometry in Monitoring Polymer Processes

- water content of resins
- colour in polymer melts during extrusion
- antioxidants in polyethylene melts during extrusion
- thickness of coatings on polyester films
- polymer blend composition

Near infrared (NIR) spectroscopy is capable of determining chemical composition. It encompasses the range of the electromagnetic spectrum from 780 nm to 2526 nm. The concentration of titanium dioxide (TiO_2), a white inorganic filler, in molten polyethylene terephthalate (PET) has been monitored¹⁹ through near infrared spectra. The spectra were collected in-line by using a flow cell, housing two fibre optic probes and mounted downstream of the extruder. Similarly, polystyrene and polyphenylene oxide blends have been monitored²⁰ through the flow cell. The flow cell has a variable path length (1 to 9 mm), and a temperature and pressure control unit to regulate the conditions inside the cell. In order to monitor the molten polymer, robust probes have been constructed^{19,21} which are capable of withstanding the rigorous process environment typical of a polymeric process such as high temperatures, high pressures and adverse chemical conditions.

On-line ultraviolet (UV) spectroscopy has been used to analyze both primary and secondary antioxidants in a polymer melt¹⁸. Antioxidants, or stabilizers, are blended with the polyolefin to reduce oxidation due to light, heat or stress. The wavelength range of UV light is 200 nm to 380 nm. UV spectra were collected, in the above case, from a sampling cell attached to the extruder die. The probes were fabricated from stainless steel with sapphire windows/lenses to tolerate the process environment. By correlating the quantity of an additive with a characteristic absorption band in the UV spectrum, on-line analysis by UV spectroscopy can be conducted to effectively monitor polyolefin additive levels.

In-line fluorescence spectrometry has been applied²² to monitor the onset of polymer

solidification during injection moulding. An optical sensor consisting of a bifurcated optical fibre, (to transmit excitation light to and collect fluorescence light from the mould cavity), was used to detect the characteristic fluorescence radiation from a dye which had been doped into the resin at a low concentration. The sensing end of the optical cable was separated from the injection mould by a sapphire optical window. Through measuring changes in fluorescence intensity it could be determined if the state of the resin was liquid or solid. Injection moulding of a glass forming polymer, polystyrene, and a crystallizable polymer, polyethylene, was monitored by this method.

2.2.3 PARTICLE IMAGING FOR MONITORING POLYMER PROCESSING

While there has been much activity concerning on-line particle size determination by methods other than imaging,^{23,24,25} there are only two reported cases in the literature where imaging has been applied on-line in a polymer processing operation.

In one case, on-line optical microscopy has been used to evaluate morphologies of immiscible polymer blends from the melt stream of a compounding process²⁶. This on-line measurement technique employs reflected light optical microscopy in conjunction with a high temperature and high pressure flow cell, a CCD (charged coupled device) camera, and an image processing and analysis system. Immiscible blends of low density polyethylene and polystyrene were studied. Particle sizes as small as 1 μm could be observed.

The second case involves a commercially available instrument, the Flow Vision Continuous On-Line Analyzer.^{7,8,9,27} This is a visible inspection system that monitors

computer enhanced images of impurities in a polymer melt stream, on-line. Light is transmitted through the polymer stream and particle images are detected on the other side. These images are converted to video and are analyzed for particle presence and size in real time by a computer. Particles such as gels, metals, fibres, black specs and filler agglomerates can be observed. The detection limit for particles is 10 to 1000 μm . Interaction with the hot, high pressure polymer is conducted through the use of specially fabricated high temperature fibre optics and high pressure optical windows. The fibre optic probes are used to convey the illumination into the polymer stream and to collect the image from the stream.

Two computers operate in real-time to process the images. The first computer, an image enhancer, separates the moving particles from the molten background. The second computer, the polymer event detector, scans the enhanced image and counts and classifies the particles into five different ranges, according to size (diameter), every one minute. This system will not identify or categorize the particles by type.

2.3 MELT FILTRATION

Melt filtration is a process in which molten polymer is forced through screens of fine openings in order to remove foreign particles. In melt filtration a screen is fitted between the end of an extruder screw and the extrusion die to capture material that does not melt at the processing conditions of the polymer. The screen also helps to build up and maintain back pressure to assist plastication and give a more homogeneous melt. This technology is particularly useful for screening out metals, papers, fibres and incompatible polymers of higher melting temperatures. Melt filtration of waste plastic has been shown to be efficient in removing contaminants to yield high properties, (based on tensile and izod impact strength),

compared to unfiltered material.²⁸

There are two modes of melt filtration: continuous and discontinuous. An example of discontinuous melt filtration is the slide-plate screen changer, as shown in Figure 3. The pressure drop across the screen is continuously monitored. When the pressure drop exceeds a certain value a hydraulic piston moves the breaker plate with the screen pack out of the polymer melt stream and concurrently replaces it with a breaker plate and a fresh screen.

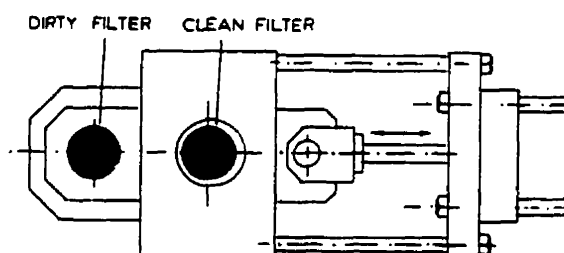


Figure 3: Slide-Plate Screen Changer

The drawback of discontinuous screen changers is that a considerable pressure drop develops across the screen before the screen is changed. This results in gradual rises and sudden drops in head pressure and melt temperature which in turn disrupts the continuous nature of the extrusion process. Figure 4 depicts a typical pressure profile of a continuous and discontinuous melt filtration system. The advantage of the continuous system is that a constant pressure drop is maintained across the filter.

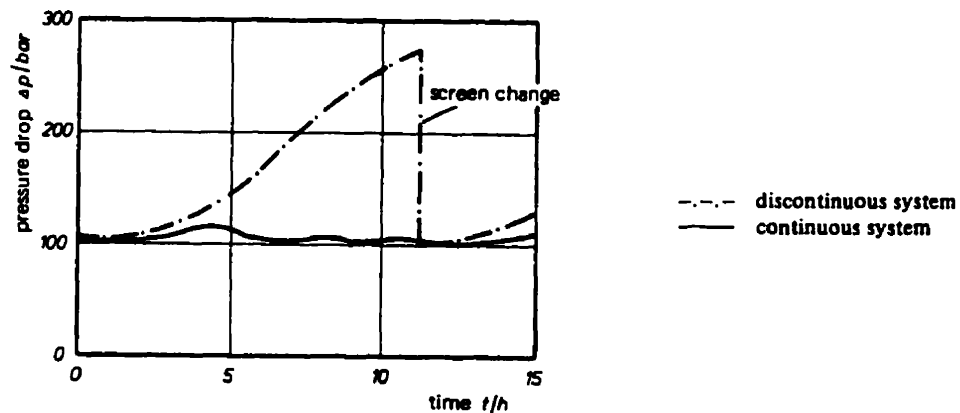


Figure 4: Pressure Profile for a Typical Discontinuous and Continuous Melt Filtration System

A continuous screen changer is shown in Figure 5. A steel ribbon filter moves slowly across the melt stream in a continuous manner. Screen movement occurs by the pressure drop across the screen; the higher the pressure drop the more lateral force will be exerted on the screen. The filter enters and then leaves the machine through water cooled blocks attached to both sides of the screen changer body. Inside these water cooled blocks the polymer solidifies and forms a seal. As the screen advances, a small quantity of polymer is allowed to exit with the screen in a controlled fashion to carry the contaminants out and provide a seal. The screen can be set to advance incrementally based on regular time intervals or based on a set pressure drop across the screen.

Recently, filtration devices have been developed that employ laser-drilled drums²⁹ in place of typical screen packs. The holes are highly concentrated on the filtration medium and are equivalent in filtration to 100 to 150 mesh screens. Particles trapped on the surface of the

holes are wiped away by mechanical arms and are removed.

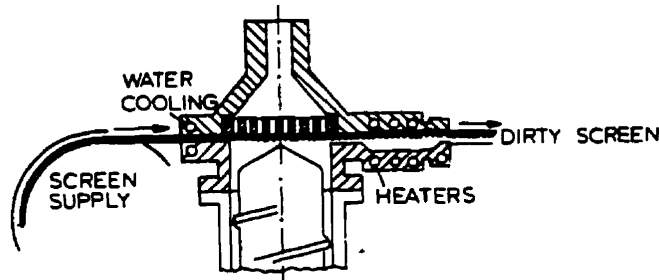


Figure 5: Continuous Screen Changer

Attempts have been made to mathematically model the melt filtration process^{3,30} in order to predict the pressure drop across the screen under different operating conditions (screen size, temperature, shear rate). It is, however, difficult to specify a filtration process in advance because usually the size and shape of the separated particles and the porosity of the filter cake in relation to the pressure are not known. This is why filter performance is always assessed experimentally.

2.4 RESIDENCE TIME DISTRIBUTION

The residence time distribution, (RTD), is a measure of the length of time that polymer spends in an extruder. It provides valuable information about the details of the conveying process in the extruder. The time material spends in an extruder has a direct effect on the quality of the product, degree of mixing, efficiency of chemical reaction and the extent of degradation. The actual conveyance of the polymer melt in an extruder rests between the

two extremes of perfect plug flow and ideal mixing.

The RTD can be measured experimentally by using a standard stimulus response technique. In this work the response to a pulse input of tracer is of interest. The residence time distribution function $E(t)$, describes the response of an extruder to such a stimulus. This function represents the age of the distribution of the polymer leaving the extruder. Since all the tracer material enters the extruder at the same time ($t=0$), the fraction of material leaving the extruder with a residence time between t and $t+dt$ is given by $E(t)dt$. The residence time distribution function, $E(t)$, can be obtained by dividing the concentration, at any time interval, by the total amount of tracer injected³¹:

$$E(t) = \frac{C(t)}{\int_0^t C(t) dt} \quad (2.4)$$

where $C(t)$ is the tracer concentration at time t .

The cumulative RTD function is defined as³¹:

$$F(t) = \int_0^t E(t) dt \quad (2.5)$$

The first moment about the origin is a measure of the mean residence time of the polymer in the extruder³¹:

$$\bar{t} = \int_0^{\infty} t \cdot E(t) dt \quad (2.6)$$

$E(\theta)$ and $F(\theta)$ are the corresponding RTD distribution functions when normalized time, θ , is used. These functions are related to $E(t)$, $F(t)$ and t as follows³²:

$$E(\theta) = \bar{t} \cdot E(t) \quad (2.7)$$

$$F(\theta) = F(t) \quad (2.8)$$

$$\theta = \frac{t}{\bar{t}} \quad (2.9)$$

The second moment about the mean, is called the variance, σ_t^2 . It is a measure of the spread of the distribution about the mean³¹:

$$\sigma_t^2 = \int_0^{\infty} (t - \bar{t})^2 \cdot E(t) dt \quad (2.10)$$

The dimensionless variance, σ_θ^2 , is described as³¹:

$$\sigma_\theta^2 = \frac{\sigma_t^2}{\bar{t}^2} \quad (2.11)$$

For the idealized case of plug flow and perfect mixing flow, the dimensionless variance takes the value of 0 and 1 respectively. For a real system σ_θ^2 varies in the range:

$$0 < \sigma_\theta^2 < 1 \quad (2.12)$$

The value of σ_θ^2 allows an approximate comparison between different distributions to be made. It does not characterize the skewness of the distribution. The skewness factor is

defined from the third moment about the mean, and the dimensionless standard deviation, by the following expression³¹:

$$As = \frac{\int_0^{\infty} (t - \bar{t})^3 \cdot E(t) dt}{\sqrt{\sigma_0^2}} \quad (2.13)$$

A major advantage of normalized residence time distribution curves is that conveying characteristics of different extruders can be directly compared.

3.0 DEVELOPMENT OF THE IN-LINE PARTICULATE VISION MONITOR

The development of an in-line particulate vision monitor that operates in real time with an extruder to optically detect and quantify particulate contaminants present in recycled plastic waste, will be described in this chapter. It is a video based instrument in which a fibre optic light guide and fibre optic image guide interact with the polymer melt to image contaminants as they flow through the extruder. Particles can range in size from 10 to 1 000 μm . A schematic of the system is illustrated in Figure 6. The high pressures (7 to 70 MPa) and high temperatures (120 to 425°C) encountered in the extrusion of polymers present a unique sample interfacing challenge.

The in-line particulate vision monitor is comprised of two parts. The first part being the interface. The interface is a piece of equipment that allows the fibre optic probes to monitor the flow. The second part consists of the illumination, detection and image analysis system. Each part will be addressed in turn in the following sections.

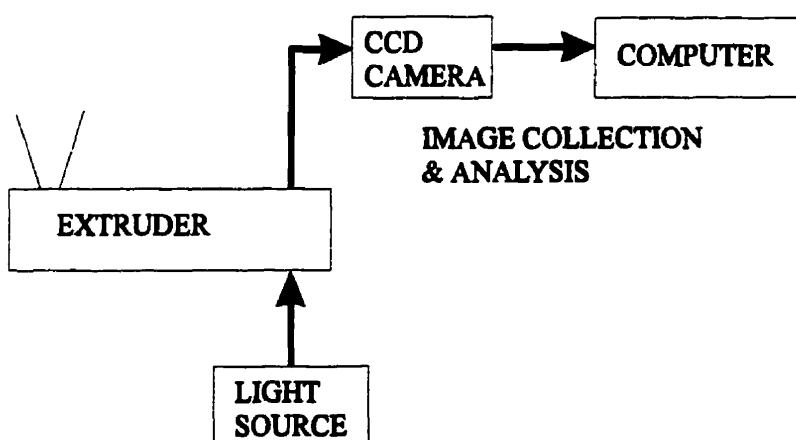


Figure 6: Overview of In-Line Particulate Vision Monitor

3.1 INTERFACE DESIGN

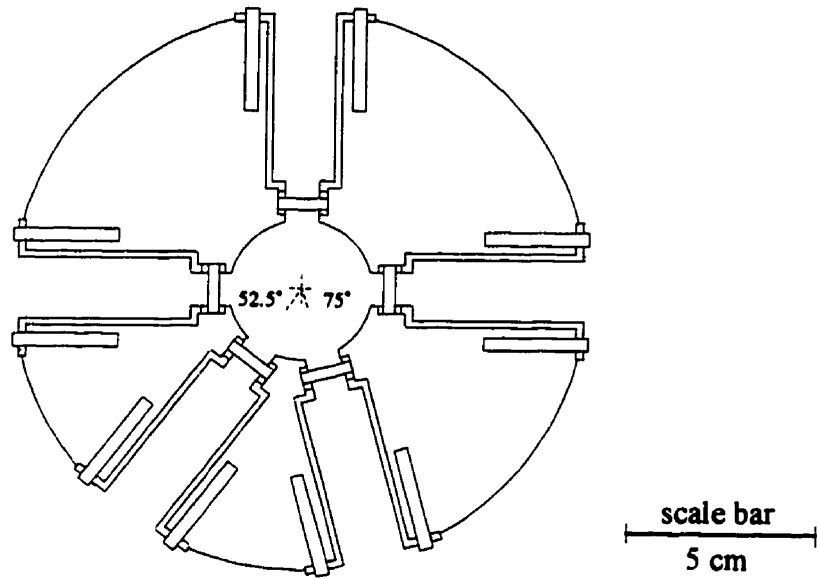
The interface permits the fibre optic probes to monitor the extrusion process in a non-invasive manner. Several major obstacles must be overcome in designing a suitable interface. First, the interface must be able to handle melts continuously at high temperatures and pressures, and deal with a wide range of viscosities. Second, the interface must ensure that the optical system will be capable of steady, reliable operation directly in the harsh extrusion environment.

Two interfaces were designed and constructed: a five-window cylindrical interface and a die strand interface. The five-window interface was a prototype and led to the development of the die strand interface.

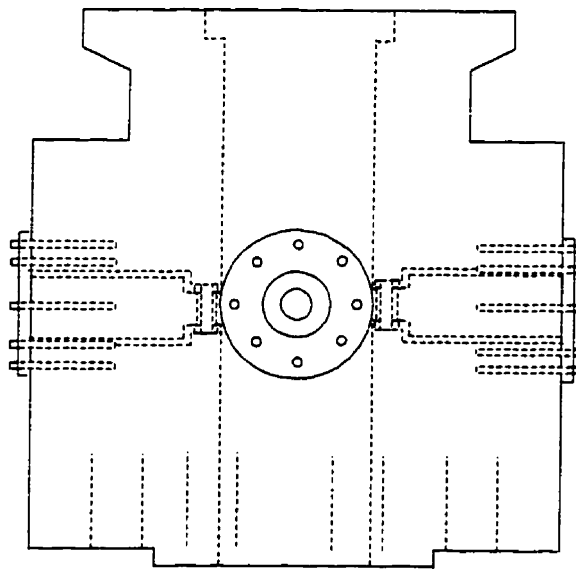
3.1.1 FIVE-WINDOW CYLINDRICAL INTERFACE

The five-window cylindrical interface, as illustrated in Figure 7, was designed to monitor the polymer flow between the end of the extruder screw and the die. The laboratory extruder used was a Deltaplast single screw extruder with a diameter of 38 mm and a length to diameter ratio of 24:1. Thus the inner diameter of this interface was designed to be 38 mm in order to maintain the polymer flow pattern. The interface was machined from steel.

To overcome the high pressure, a sapphire window was chosen as the medium to separate the flowing polymer from the optical probe. Sapphire was chosen because it is transparent, has a high Young's modulus value, (370 GPa), possesses extreme surface hardness (Moh hardness =9), and is chemically inert. Sapphire also has high light transmission, 85%, in the visible range. Based on standard formulas for stress and strain³³, it was determined that a 2 mm thick sapphire window with a 127 mm diameter, (fixed-edged



Front View (centre cross-section)



Top View

Figure 7: Five-Window Cylindrical Interface

plate and loaded uniformly), could adequately withstand a pressure of 70 MPa, and not fail in tension.

Because sapphire is brittle, the sapphire window was fitted between two copper gaskets, each 0.8 mm thick. To hold the window assembly in place, pressure was applied to the outer edge of the window through a collar insert that was held in position by 8 screws (size no.4, fine thread series). The actual fibre optic probe could then be inserted into the collar and face the window.

Based on off-line experiments conducted with a hot stage equipped Nikon Labophot microscope, it was concluded that opaque particles could be adequately viewed under transmitted light conditions, (i.e. light source and detector at 180° to each other). While particles having a similar refractive index to the polymer, such as gel, achieved suitable contrast with the background under scattered light conditions. Under scattered light, particles are illuminated from the side with a beam of light, and at an angle to the detection system's optical axis. It was thus proposed to introduce 5 windows about the periphery of the cylindrical interface, allowing the monitor to operate under both transmitted and scattered light conditions.

Because the fibre optic image guide has a maximum operating temperature of 120°C, (above 120° C the epoxy that is used to hold the aligned optical fibres in place starts to soften), a double pass cooling jacket was designed to line the inner wall of the collar in order to maintain the probe at room temperature. Water was used as the cooling medium. In addition, two band heaters, (450 W each), were used to heat the interface.

Once implemented on the laboratory extruder, there were two major problems associated with this interface. The first problem concerned the presence of a stagnant polymer layer, about 2 mm thick, which formed immediately outside the sapphire window. This resulted from the fact that the window was recessed 2 mm from the main wall of the cylindrical flow chamber and consequently it was difficult to observe the polymer flowing behind this stagnant layer. The window was recessed in order to have metal support to hold the window in place.

The second problem that hindered the use of this interface was the fact that the polymer, at a thickness of 38 mm, was too opaque under normal operating conditions. Light was not easily transmitted through the polymer. Recycled high density polyethylene (HDPE) was the material used and it was extruded at temperatures ranging from 180°C to 250°C.

It was postulated that a temperature gradient inside the flow channel contributed to the opaqueness of the polymer melt. Because polymers are good insulators, the development of a temperature gradient across the flow cross-section was feasible. Therefore static mixers, which are used for thermal mixing to achieve temperature homogenization, were placed before the interface. Two Koch static mixers having a diameter of 38 mm and a total of 12 mixing elements were used. The static mixers, however, did not improve the clarity of the recycled HDPE.

This interface did operate with virgin linear low density polyethylene (LLDPE) at 200°C; but a 50/50 blend of virgin LLDPE/ recycled HDPE still appeared opaque. Only at a temperature of 475°C, (which is well above normal operating conditions), did the recycled HDPE become optically clear. The optical clarity was most likely due to polymer

degradation. It is known that breakage of HDPE polymer chains occurs above 300°C.

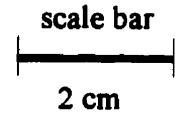
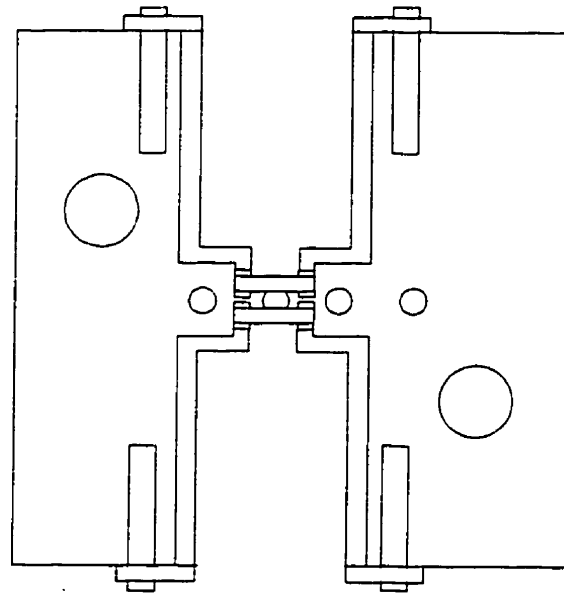
Based on the above experience, it was decided that a smaller path length (i.e. polymer thickness) would be required in order to view particulate matter in recycled HDPE. This prompted the development of the second interface, the die strand interface.

3.1.2 DIE STRAND INTERFACE

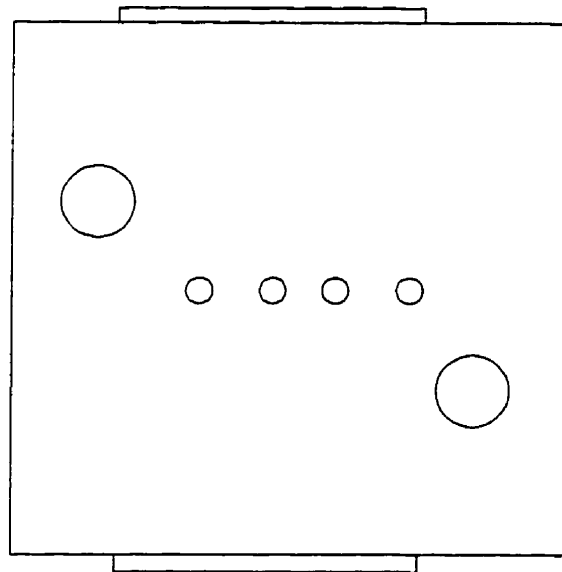
The die strand interface, as illustrated in figures 8 and 9, is fabricated from steel and is bolted onto the end of the extruder die. It is an extension of the die and consists of four narrow flow channels, each 3 mm in diameter. A selected centre strand is monitored. A sapphire window is situated above and below this selected strand; the sapphire windows are directly opposite one another. Each window protrudes 0.5 mm into the flow channel, to preclude the formation of a stagnant polymer layer. The polymer thickness, (path length), between the two windows is 2 mm. This configuration permits the interface to operate only in the transmitted light mode. The light guide illuminates the polymer stream through the bottom window and the image is detected from the top window.

The same design principles were adhered to in designing the die interface as with the previous interface. The window thickness, collar design and cooling jacket were identical. This interface was heated through conduction from the die.

High magnification, about 400x, coupled with a high linear velocity of the particles past the sapphire window resulted in image distortion each time an image of the recycled HDPE was captured through the computer. At a shutter speed of 1 ms, the image of the moving particles appeared blurred. To overcome this problem a toggle clamp assembly was

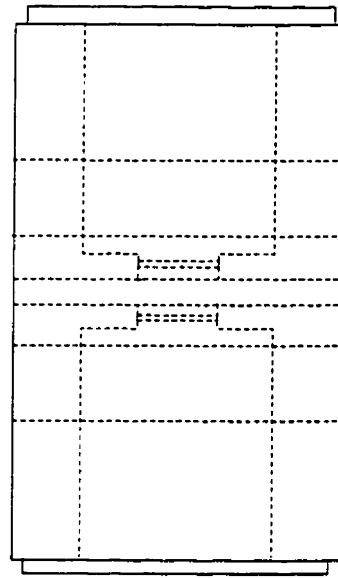


Front View (centre cross-section)



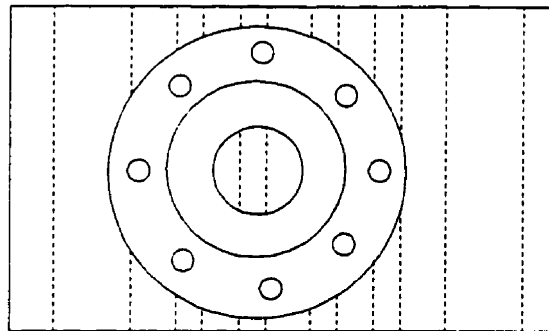
Front View

Figure 8: Die Strand Interface: centre cross-section and front view



scale bar
2 cm

Side View



Top View (and Bottom View)

Figure 9: Die Strand Interface: side, top and bottom view

mounted onto the side of the interface. A manually operated plug with a conical teflon nib could be used to stop the flow of the strand being monitored, for 1 s, in order to allow a clear, unblurred image to be captured.

It is possible to focus on different strata in the flow channel with the imaging system by varying the distance between the objective lens and the sapphire window. With laminar flow the velocity profile is parabolic. The maximum velocity can be observed at the centre with lower velocities occurring near either window. Typically the central portion of the stream is monitored.

3.2 IMAGE FORMATION AND ANALYSIS

The second part of the in-line particulate vision monitor involves the illumination, detection and image analysis system. Figure 10 illustrates the arrangement of these components.

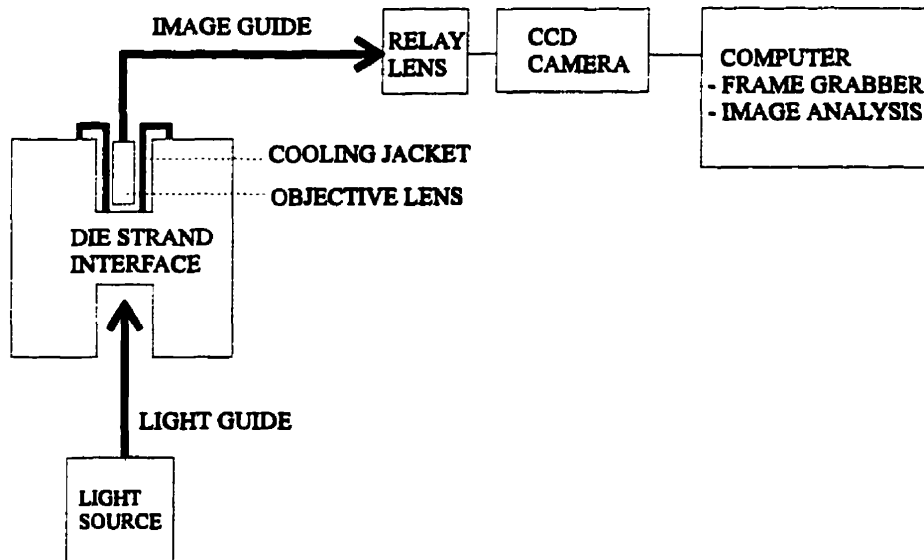


Figure 10: In-line Particulate Vision Monitor

The polymer stream, travelling through the die strand interface, is illuminated by a quartz light guide which is connected to a 150 W quartz halogen lamp. An objective lens situated at the distal end of the image guide focuses the image of the polymer stream onto the active area of the image guide. The fibre optic image guide then transmits the image to a CCD (charged coupled device) camera which transforms the image into a standard analogue video signal. At the end of the system, a 486 computer equipped with a frame grabber, (an analogue to digital converter), and image analysis software, (Global Lab Image 2.0), is used to conduct image processing and analysis, and to generate particle size distributions.

Detailed descriptions on the above equipment are provided in Appendix A.

3.2.1 IMAGE PROCESSING AND ANALYSIS

Through image processing and analysis the images of particulate contaminants present in recycled plastic waste can be quantified. Image processing involves the various operations which can be performed on the image data. These operation include preprocessing, spatial filtering, image enhancement and feature detection. Images are typically represented using a two dimensional array of picture elements (pixels). Each pixel in the image takes on a value that indicates the strength of the signal at that location. In a black and white image the range of quantization values is called the greyscale. The range begins with black, or zero, and increases to 255, white, with lighter and lighter shades of grey. The individual quantization values are called grey levels.

The particular image processing and analysis techniques used to process the images of particulate contaminants will be fully addressed in the results and discussion section.

3.3 NOVELTY OF THE IN-LINE PARTICULATE VISION MONITOR DESIGN

The novel aspect of the In-Line Particulate Vision monitor design centres on the die strand interface. The strategic location of this interface coupled with the flexible, non-intrusive manner in which it allows normal probes to easily interact with a polymer processing stream, operating at elevated conditions of pressure and temperature, are unique. Owing to the open collar design and the method of securing the sapphire window at the base of the collar adjacent to the flow, the die strand interface is able to accommodate various types of probes that will allow for chemical and physical measurements to be performed. A cooling jacket can line the inside of the collar in the case of temperature sensitive probes.

Not only has imaging and quantification of particulate contaminants been accomplished through this device,³⁴ (the topic of this thesis), but this interface has also been employed to image polyethylene/polystyrene blends.³⁵ In addition, a near infrared probe has been used in conjunction with the die strand interface to monitor the chemical composition of recycled high density polyethylene and polypropylene blends,^{36,37} and to perform in-line colour measurements of pigmented polyethylene during extrusion.³⁸

Previous attempts to monitor polymer processes via fibre optics have been conducted on-line, in a sample stream, through the controlled conditions of a flow cell. Furthermore, robust probes capable of withstanding the harsh environment of a polymer process had to be constructed in these situations. This involved developing a protective housing for the probe and affixing a sapphire window to the tip of the probe. Specific examples of the above attempts have been cited previously in section 2.2.2., Fibre Optic Assisted

Spectrophotometry in Monitoring Polymer Processes. The advantage of the die strand interface, on the other hand, is that it readily accommodates ordinary probes, without modification, to monitor a polymer process.

4.0 EXPERIMENTAL PROCEDURES

4.1 UTILITY ASSESSMENT OF THE PARTICULATE VISION MONITOR

The utility of the particulate vision monitor for monitoring the quality of recycled plastic waste was accomplished through the in-line evaluation of four different grades of recycled polyethylene (PE). A diagram of the experimental setup is shown in Figure 11.

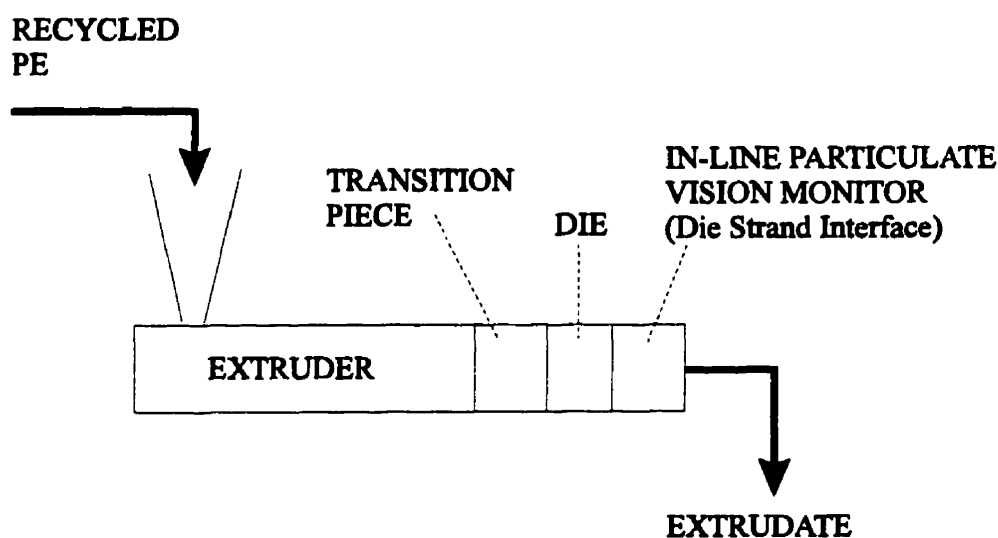


Figure 11: In-Line Evaluation of Recycled Polyethylene

A Deltaplast single screw extruder with a diameter of 38 mm and a length to diameter ratio of 24:1 was used to extrude the recycled PE. The extruder was equipped with a general purpose mixing screw and a four strand die, (3 mm openings). The die strand interface, with the corresponding illumination, detection and image analysis system, was affixed to the end of the die.

The extrusion system, (extruder, transition piece and die), had 5 temperature control zones. Three zones provided heating and cooling for the extruder barrel and two zones consisted of heating via band heaters for the transition section and die. The feed throat of the extruder was water cooled. Pressure was monitored at the screw tip and after the breaker plate in the transition section.

Recycled plastic was introduced into the hopper and was extruded at a constant temperature of 200°C and at a screw speed of 30 rpm. Upon reaching steady state, 20 individual images were captured and saved, for each polymer batch, with the image analysis software, Global Lab Image 2.0. One image of the particulate contaminants was captured every 30 s. (In addition to capturing images through the image analysis software, it was also possible to record the polymer flow continuously on video tape). The extruder was purged with virgin HDPE after each polymer batch was extruded.

The material which was evaluated consisted of 3 batches of unpigmented, pelletized, blow-moulding grade, post consumer recycled high density polyethylene (HDPE). Each batch had been obtained from a different vendor. The recycled HDPE had been previously filtered through screen packs consisting of a Dutch weave stainless steel screen. The fourth polymer batch which was evaluated, consisted of recycled, pelletized stretch wrap. Stretch wrap is composed of 97% low density polyethylene (LDPE) and 3% polyisobutylene. This material had been filtered through a laser-perforated filter. Details on the four polymer batches are summarized in Table 4-1.

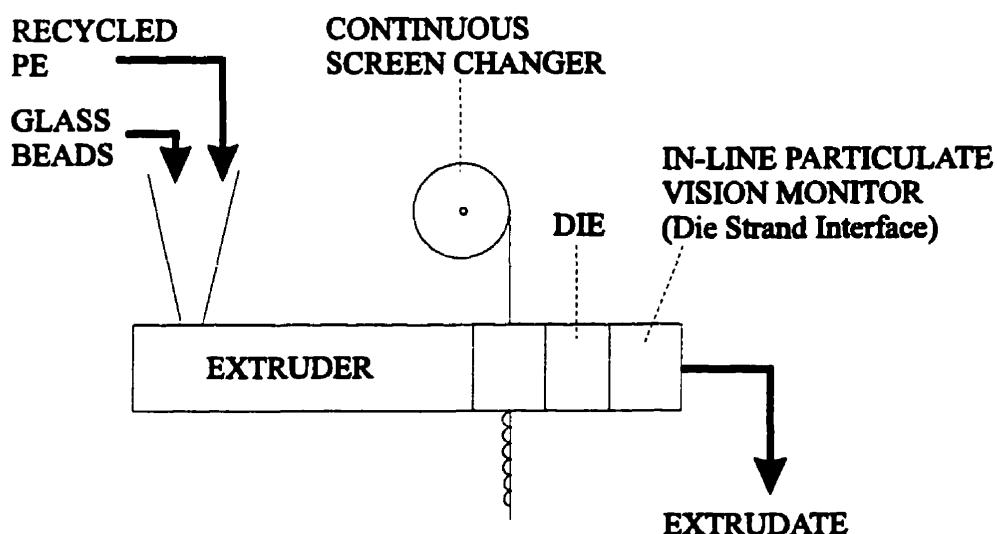
TABLE 4-1: Recycled Polyethylene Evaluated In-Line

PE batch	Filtration Method	Mesh Size	Aperture (μm)	Melt Flow Index (g/10 min)	batch size (kg)
A-HDPE	screen pack (Dutch weave screen)	110	140	0.68	500
B-HDPE		120	122	0.53	500
C-HDPE		125	120	0.62	50
D-LDPE	laser filter	-	100	1.27	50

In order to calibrate the detection system, to determine the magnification achieved, a 1g pulse of 250 μm diameter monodisperse glass beads was injected into the feed port of the extruder by an air gun.

4.2 ASSESSMENT OF MELT FILTRATION

Melt filtration was evaluated in-line through both transient and pulse response testing techniques. A HITECH continuous screen changer was used to remove foreign particles present in the polymer melt. Figure 12 depicts the equipment arrangement employed.

**Figure 12: In-Line Evaluation of Melt Filtration**

The melt filtration unit had its own temperature control zone and cartridge heaters. It was also possible to monitor the pressure drop across the screen.

4.2.1 TRANSIENT TESTING

In transient testing, a filter cake was allowed to develop on the filter screen over a duration of six hours. The screen was not advanced for this period of time. Recycled HDPE was passed continuously through the extrusion system, as illustrated in Figure 12, for 6 hrs. Every 1 hr, 10 images of the filtrate were captured at a rate of 1 image/ 20 s, with the in-line particulate vision monitor. The pressure drop across the screen was recorded every 30 min.

The continuous screen changer was equipped with a reversed Dutch twilled weave screen. Transient testing was conducted at two different temperatures. Table 4-2 outlines the experimental conditions that were implemented.

TABLE 4-2: Transient Testing of Melt Filtration

Run	Material	Mesh Size	Aperture (μm)	Extrusion Conditions	
				T	rpm
1	A-HDPE	280	55	180°C	20
2	A-HDPE	280	55	220°C	20

4.2.2 PULSE RESPONSE TESTING

In pulse response testing, a small quantity of glass beads is injected into the extruder. Pulse testing is used to evaluate filtration efficiency by providing information on the glass bead size distribution both before and after the filter. It is also used to determine the residence time distribution of glass beads in the extrusion system.

A two-level factorial design having two variables, (temperature and screw speed), was implemented. Recycled HDPE, (A-HDPE), was passed through the extruder and upon reaching steady state a 5 g pulse of glass beads was injected into the extruder. Images of the glass beads were captured every 20 s for a total time of 25 min. The experimental setup is shown in Figure 12. The continuous screen changer was outfitted with a reversed Dutch twilled weave screen. Table 4-3 describes the experiments which were performed.

TABLE 4-3: Conditions for Pulse Response Testing

Run	Temperature	Screw Speed (rpm)	Mesh Size	Aperture (μm)
1	180°C	20	200	75
2	180°C	50	200	75
3	220°C	20	200	75
4	220°C	50	200	75
control				
5	180°C	20	no screen	
6	180°C	50	no screen	

Size specifications of the glass beads that were pulsed through the extrusion system are provided in Table 4-4.

TABLE 4-4: Glass Bead Size Distribution

	10%<	50%<	90%<
glass bead diameter	15 μm	62 μm	113 μm

5.0 RESULTS AND DISCUSSION

5.1 UTILITY ASSESSMENT OF THE PARTICULATE VISION MONITOR

5.1.1 IMAGE INTERPRETATION

A typical image of recycled polyethylene obtained with the in-line particulate vision monitor is shown in Figure 13. This image of recycled high density polyethylene, (A-HDPE), was acquired during extrusion at 200°C and 30 rpm. The particulate contaminants of interest are the dark irregularly shaped objects. The background of the image consists of an ordered arrangement of small squares which are due to the coherent fibre optic image guide. Each square represents a fibre bundle consisting of 25 coherent image fibres; the individual fibres have a diameter of 10 μm . Because the distal end of the image guide is located in the same plane as the focused image from the polymer stream the two objects are superimposed. As a result, the image guide structure appears as part of the polymer stream image.

The regular presence of thin black horizontal lines and short black vertical lines in the image background are caused by empty spaces between the fibre bundles. Other black marks in the background, such as the spotted horizontal line located one third of the distance from the top of the image, are due to damaged image fibres which do not transmit light and therefore appear black.

In order to quantify the information contained in such an image derived from the in-line particulate vision monitor, an interpretation algorithm was developed. The interpretation algorithm is outlined in Figure 14.

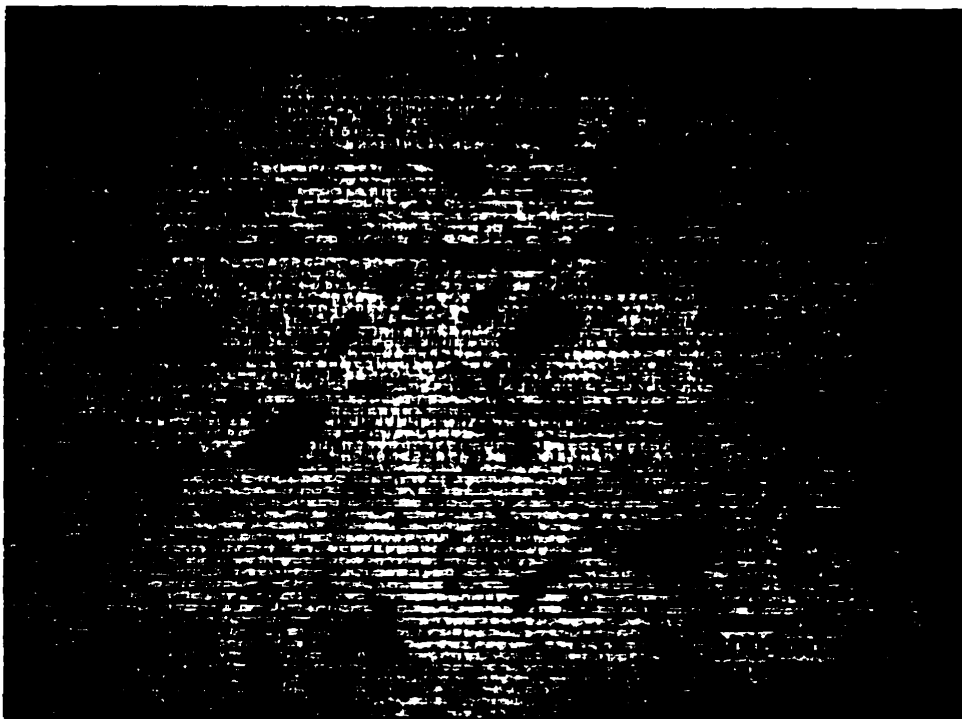


Figure 13: In-Line Image of Recycled Polyethylene (A-HDPE) During Extrusion (200°C, 30 rpm)

INTERPRETATION ALGORITHM

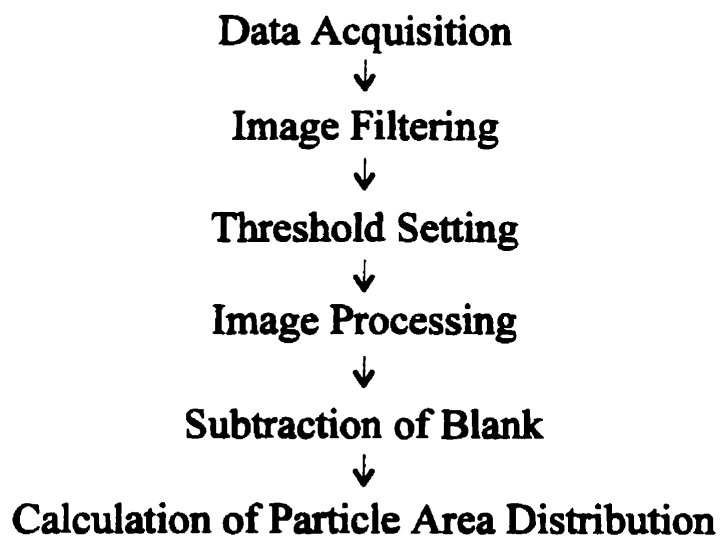


Figure 14: Interpretation Algorithm for In-Line Images

In the first step of the algorithm, the in-line image is acquired through the frame grabber and image analysis software. Next, the image is enhanced through digital filtering to elucidate the particles of interest from the background. Figure 15 shows the image of Figure 13 after it has been digitally filtered with a median filter. The net effect of the median filter is to smooth an image or reduce image noise. True discontinuities such as object borders are not broadened, shifted or reduced in contrast by the median filter. The median filter has diminished the appearance of the image guide structure and the non-uniform illumination (brightest spot is in central portion of image) in Figure 13 to yield a more homogeneous background, Figure 15.

A median filter operates by replacing a pixel value with the median value of the pixels in a given neighbourhood. The median filter works in a 3x3 pattern. The grey levels present in the pixels that define the 3x3 square are ranked in ascending order. The median value grey level, (i.e. the fifth ordered grey level value out of nine), will then replace the central pixel in the 3x3 square. This operation is performed on the entire image, always referring to the grey level values present in the original image. The median filter was applied to all images successively 5 times, since it was found that at this point no further change occurred to the image with further applications.

The appropriate grey scale threshold values are then set using the histogram minimum method³⁹ to enable the image analysis software, Global Lab Image 2.0, to classify the pixels in an image into particles and background. Proper objective threshold selection is critical to produce a tight outline around the particles, and to yield reproducible results. Two

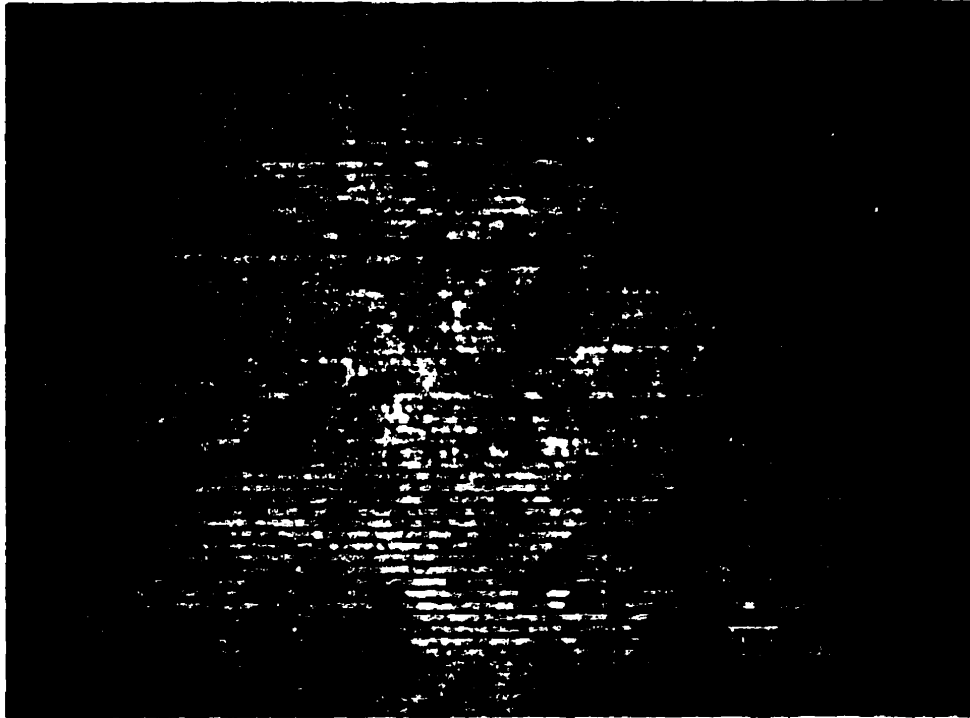


Figure 15: Median Filtered Image (median filter applied 5 times)

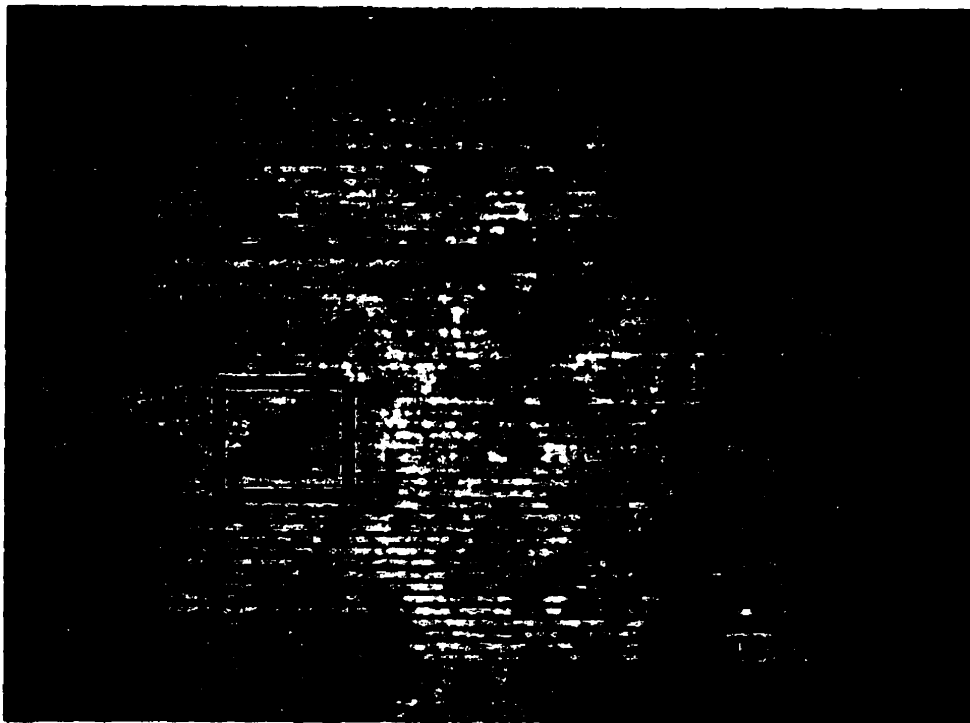


Figure 16: Histogram Minimum Method: Selected Area

threshold levels, an upper and a lower threshold level, are established. Pixels having grey level values which rest between the two thresholds are considered to be part of the features of interest, all other pixels are considered to be part of the background.

The histogram minimum method is based on a grey level histogram that is produced from a selected area on the median filtered image. The selected area contains both typical particle and background information. The black box on Figure 16 is an example of a selected area which was used to construct a grey level histogram. The resulting histogram is presented in Figure 17, as a plot of percentage of total pixels versus grey level value.

The minimum grey level value between the two peaks in the histogram is the point at which the peaks belonging to the particles and the background are most recognizably separated. The left part of the histogram corresponds to the particles of interest and the right part corresponds to the background. The upper selected threshold value is the minimum grey value between the two peaks. In the case of Figure 17, the upper threshold value is 163 on a greyscale ranging from 0 to 255.

The lower threshold value is set at black, a grey level of 0, because the particles of interest in the image belong to the dark phase of the image; whereas the background belongs to the lighter phase. Setting global grey scale threshold values for the entire image, based on a selected area of the image, assumes that there is uniform illumination throughout the image.

Calibration of the image is performed by using the 250 μm diameter of a glass bead as a scale. For each run that is conducted with the in-line particulate vision monitor, a 1 g

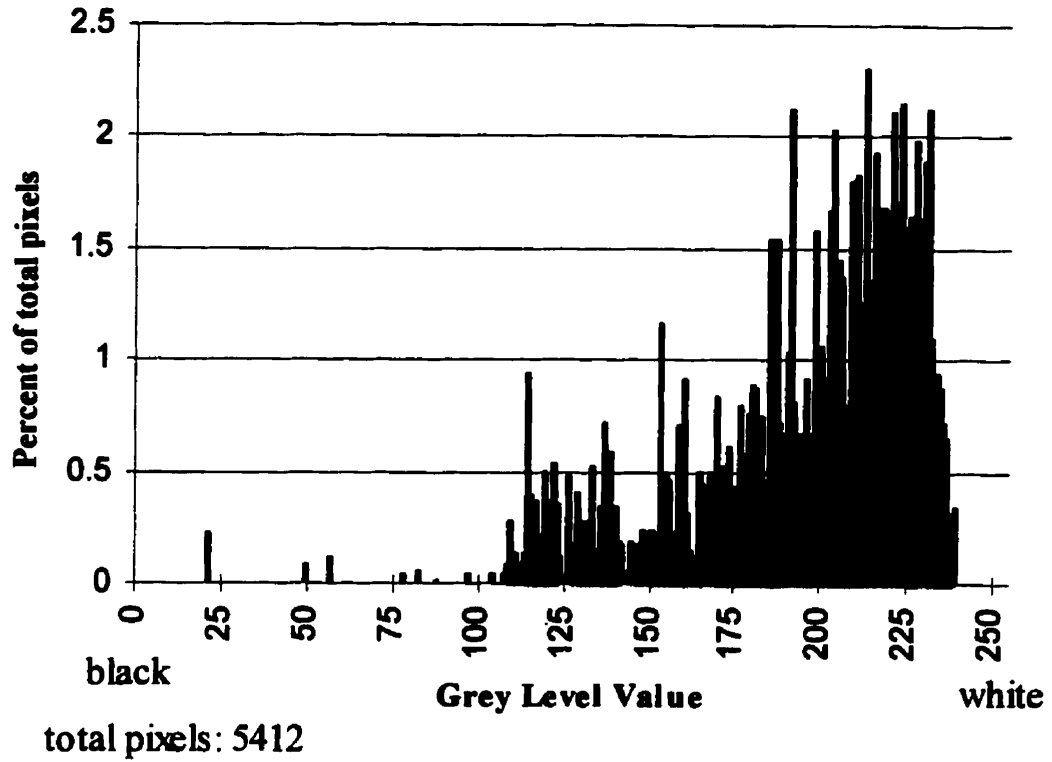


Figure 17: Grey Level Histogram of Selected Area on Figure 16

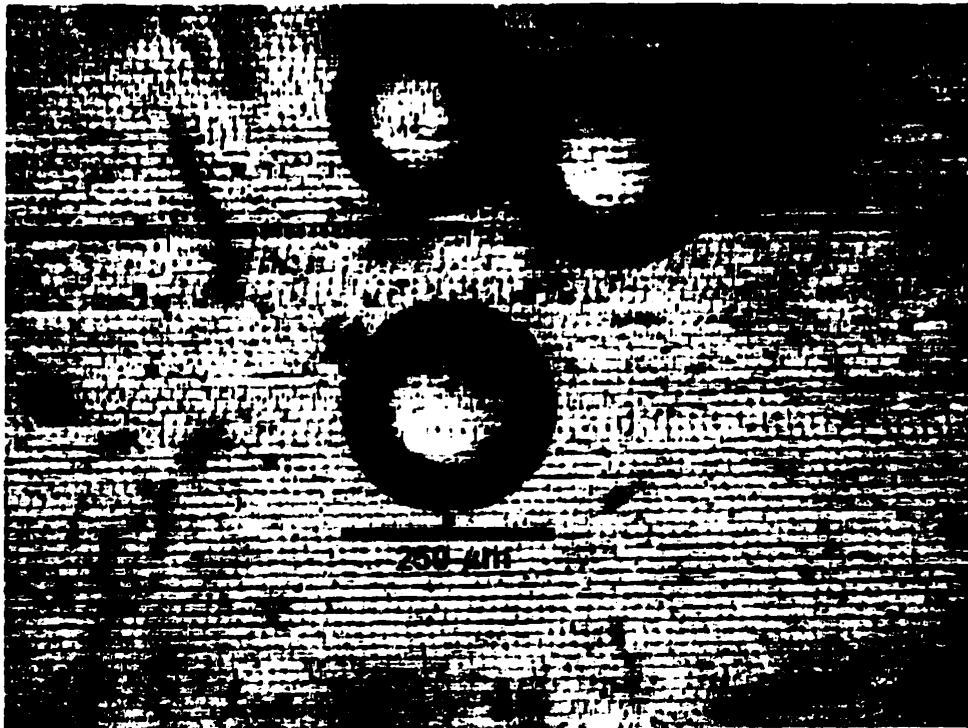


Figure 18: 250 µm Diameter Glass Beads

pulse of monodisperse glass beads, having a diameter of 250 μm , is passed through the extruder. An image of the glass beads is captured, as shown in Figure 18, and is used to determine the magnification achieved by the monitor.

Based on the threshold settings and the calibration, the median filtered image is then processed by the image analysis software. The desired information, such as projected area, length and width, is reported for each detected particle in the image. Part of the image guide structure, however, which should be classified as part of the background, will be detected as particles. These particles, which constitute the blank image, need to be subtracted from the total particles detected.

Subtraction of the blank image is accomplished by analyzing the blank image guide, (i.e. with no particles present), and accumulating information on the particles that are reported. It is this blank information which is subtracted from the actual image of the recycled polyethylene. Appendix B contains the histogram of 1 image of recycled polyethylene (A-HDPE), Figure 15, and the histogram of the blank image guide.

The processed image of Figure 15 is shown in Figure 19. The detected particles have been numbered. Particulate contaminants of interest as well as damaged image fibres, (note the horizontal line of damaged fibres one third of the distance from the top of the image), have been detected. Detected particles which are not considered to be particles of interest are removed from the data set through the subtraction of the blank.

Information on the particulate contaminants present in the image is plotted as a particle area distribution. The particle area distribution is calculated as the number



Figure 19: Processed Image of Figure 15

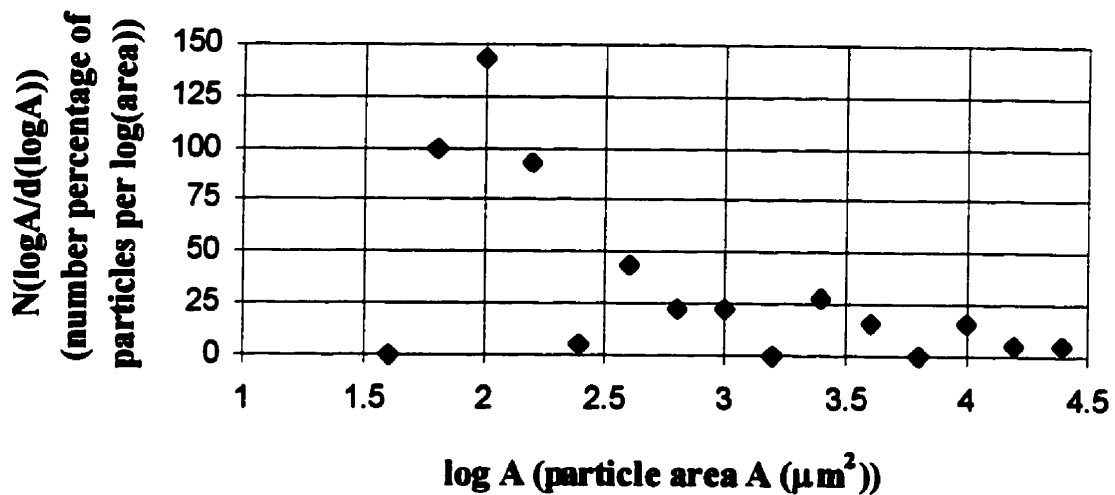


Figure 20: Particle Area Distribution of Particulate Contaminants in Recycled High Density Polyethylene (A-HDPE) Based on 1 Image

percentage of particles per $\log(\text{area})$ versus $\log(\text{area})$. The total area under such a distribution is 100 and the area between any two values on the $\log(\text{area})$ axis, $\log A_1$ and $\log A_2$, represents the percentage of the number of particles in that range. Figure 20 illustrates a particle area distribution which was generated with the information based on one image, Figure 19. Figure 19 contained 90 particulate contaminants. The tail of this distribution displays a large amount of scatter.

To determine the number of images required in order to generate a reproducible particle area distribution, the data from a series of 10 images were accumulated and the resulting distributions were plotted. Figure 21 shows the effect of accumulating images on the resulting particle area distribution. The particle area distribution generated from one image is identical to the distribution described previously in Figure 20, in which the information from one image was used to construct the distribution. With 2 images, the particle information from 2 images has been summed together. As the number of images increases the number of particles also increases.

At 3 images, scatter is prevalent in the tail and the particle area distribution is still variable. At 5 images, however, the distribution becomes stable. As the number of images is increased from 6 to 10 images a minimal change occurs to the individual points in the distribution. Based on the above analysis, a total of 10 images was chosen to reflect an appropriate sample size. This number of images corresponds to about 1 000 particles. At this sample size of approximately 1 000 particles, accurate and reproducible distributions can be generated. Sample calculations for producing a particle area distribution are provided in Appendix C.

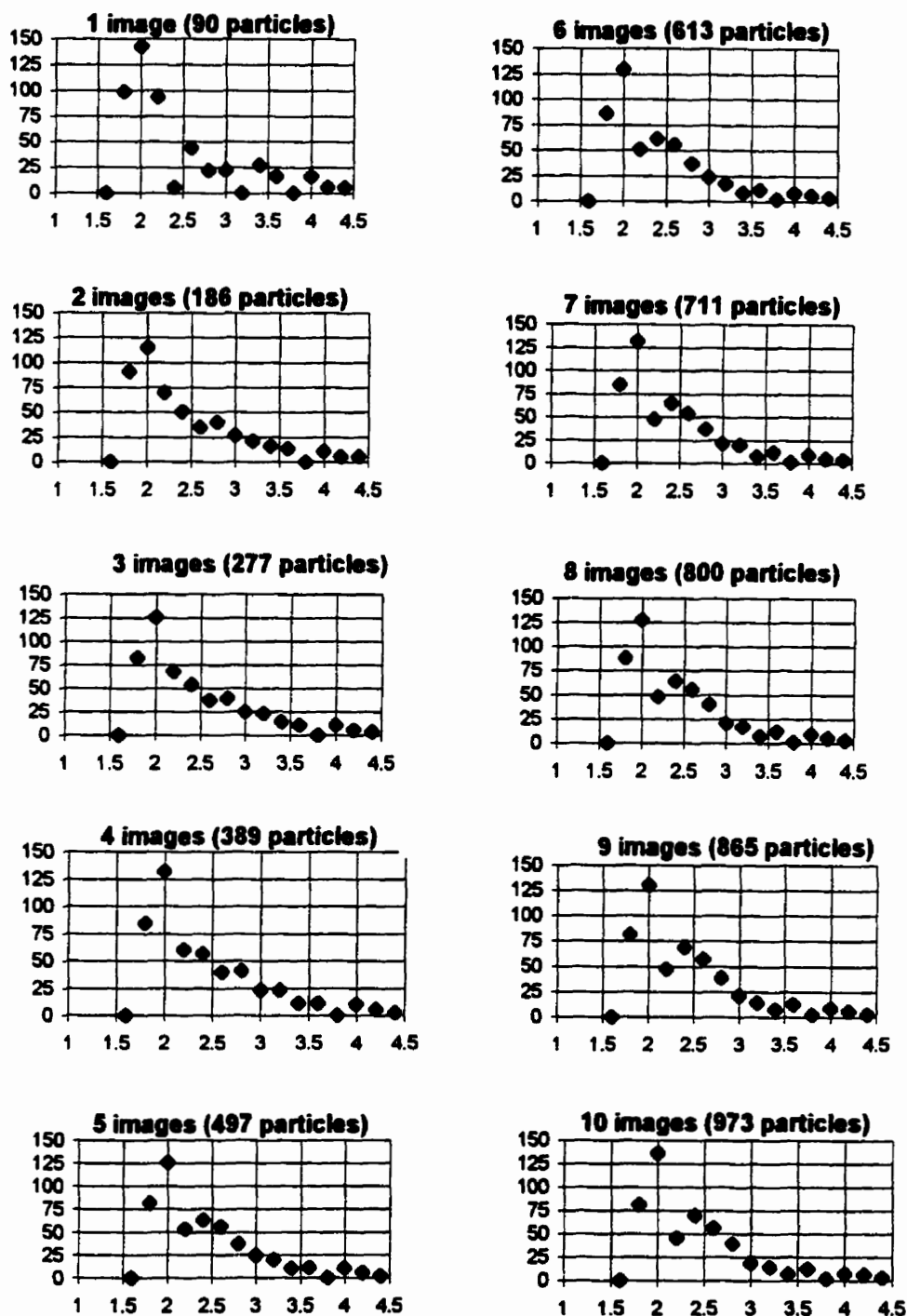


Figure 21: Effect of Accumulating Images on the Particle Area Distribution (material = A-HDPE)

x-axis: $\log A$ (particle area A (μm^2))

y-axis: $N(\log A/d(\log A))$ (number percentage of particles per log (area))

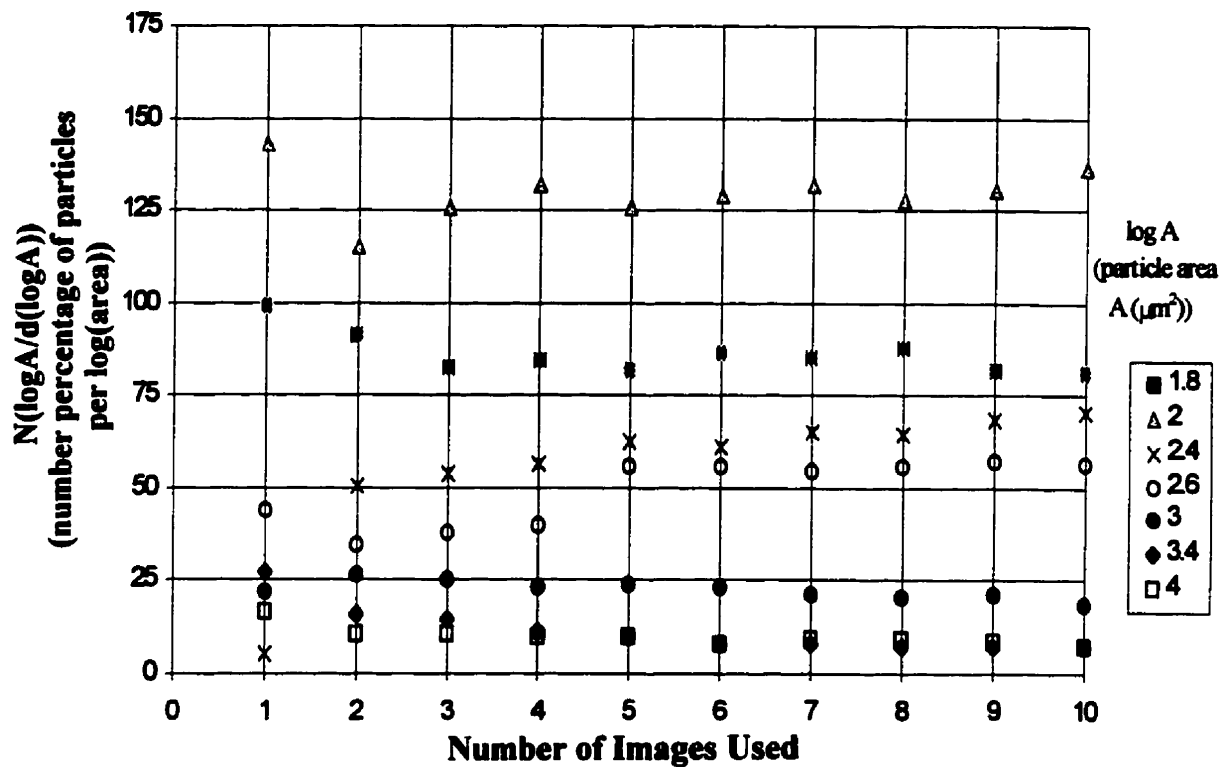


Figure 22: Height of Particle Area Distribution versus Number of Images Used (material= A-HDPE)

Figure 22 further supports the claim that the heights on the particle area distribution approach a constant value when the data from 10 images are combined. Figure 22 is a plot of the individual heights of the particle area distribution versus the number of images used. Initially, the heights corresponding to different particle areas are variable. After 5 images are combined a steady height value is attained.

5.1.2 EVALUATION OF RECYCLED POLYETHYLENE

Four different grades of recycled polyethylene were evaluated. The results from 3 types of the post consumer recycled high density polyethylene (HDPE) are illustrated in Figures 23, 24 and 25, as particle area distributions. All the material had been previously filtered through a conventional Dutch weave stainless steel screen, with screen sizes ranging from 110 mesh (140 μm) to 125 mesh (120 μm). Despite the differences in screen size used to filter the material and the different sources of the unpigmented, blow-moulding grade recycled HDPE there were strong similarities between the 3 polymer batches.

All the particle area distributions were bimodal, that is two distinct peaks were present. One peak, the larger one, occurred in the low particle area regime, (100 μm^2), while a distinct but more subtle peak appeared in the high particle area regime, (250 μm^2 to 400 μm^2). The low particle area regime is typified by small circular particulate matter such as glass chips and dirt granules. The high particle area regime is characterized largely by fibrous matter such as paper fibres which possess short width and long length dimensions, resulting in a large projected area. All batches contained particulate matter which resided in the area range of 30 μm^2 to 25 000 μm^2 .

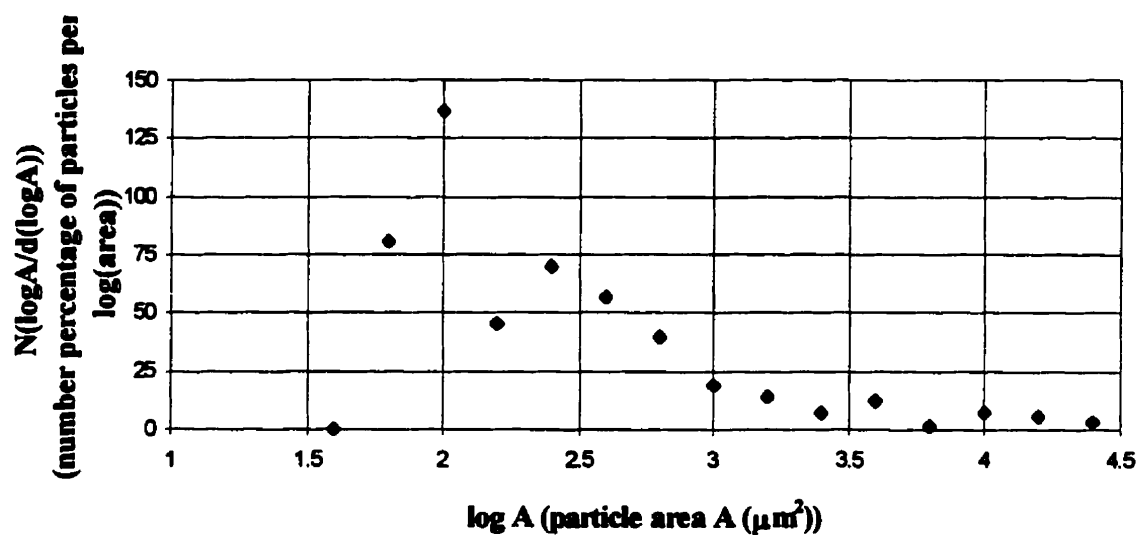


Figure 23: Particle Area Distribution of A-HDPE, 10 images

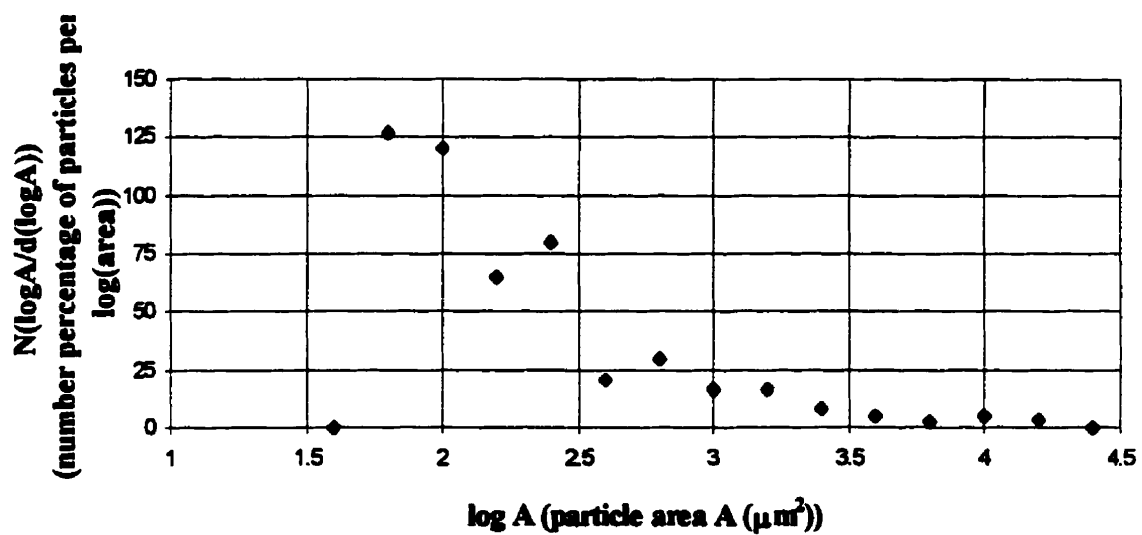


Figure 24: Particle Area Distribution of B-HDPE, 10 images

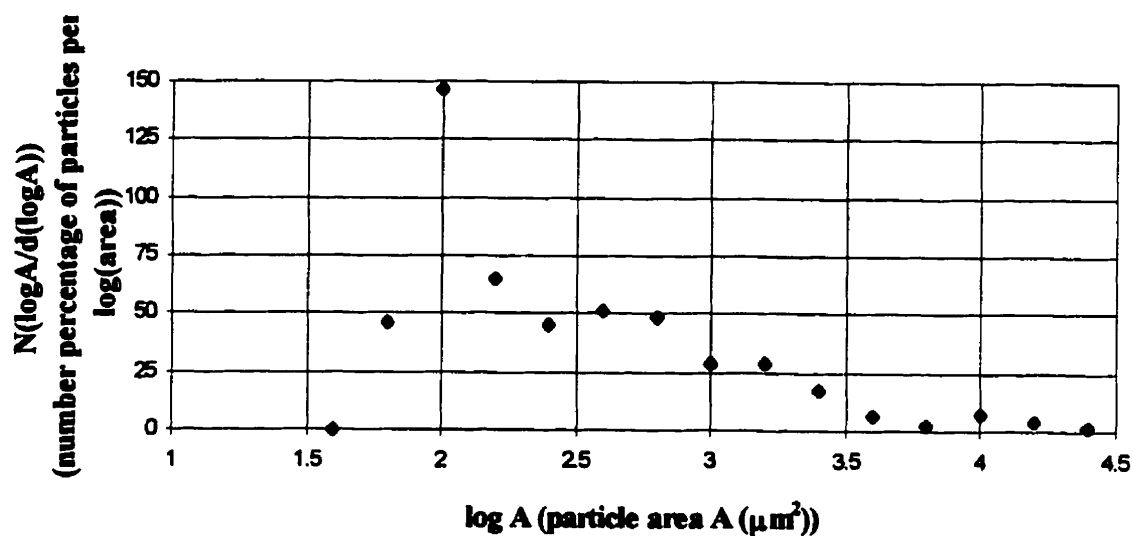


Figure 25: Particle Area Distribution of C-HDPE, 10 images

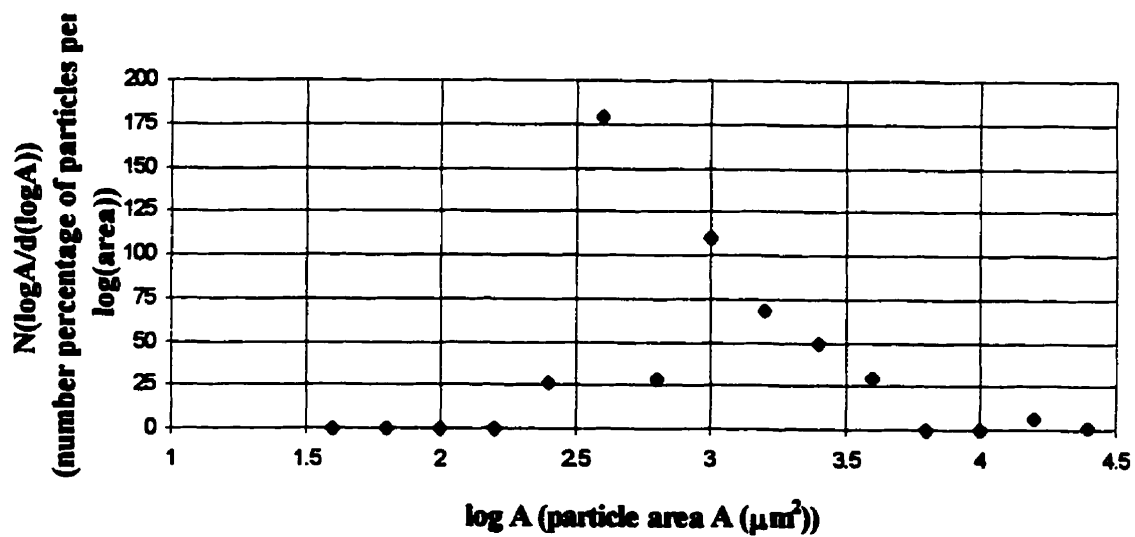


Figure 26: Particle Area Distribution of D-LDPE, 10 images

The fourth batch of recycled polymer, D-LDPE, which was evaluated, consisted of stretch wrap. Stretch wrap is a mixture composed of 97% low density polyethylene and 3% polyisobutylene. The particle area distribution for this material is presented in Figure 26. The stretch wrap had been previously filtered through a laser filter having hole openings of 100 μm . The laser filter had hole openings which were 20 μm smaller than the finest Dutch weave screen that was used in filtering the previous 3 batches of recycled HDPE.

In comparing the particle area distributions of the laser filtered material, D-LDPE, to the previous 3 batches of recycled HDPE it appears that the laser filtered material displays the highest level of particulate contamination, in terms of particle area. The particle area distribution of the stretch wrap material, D-LDPE, is shifted to the right, compared to the previous 3 batches of recycled HDPE. With the stretch wrap material, the first peak occurs at 400 μm^2 in the low area regime. In contrast, it is at this area, 400 μm^2 , where the second peak is situated for C-HDPE in the high area regime of the distribution.

However, a micrograph of the stretch wrap material, Figure 27, acquired off-line at 200°C with a hot-stage equipped optical microscope, reveals that this material possesses a minute contamination level. Furthermore, the material is homogeneous as compared to the 3 previous batches of recycled HDPE, filtered through a Dutch weave screen. In-line and off-line images of recycled high density polyethylene are contained in Appendix D.

The largest particles in the recycled stretch wrap, D-LDPE, appear as elongated cylinders having a width of 20 μm and a length of approximately 400 μm . The laser filter may be responsible for the shape of these particles. The identity of these particles could be



Figure 28: In-Line Image of D-LDPE During Extrusion (200°C, 30 rpm)



Figure 27: Off-Line Image of D-LDPE (200°C, transmission illumination)

paper fibres that have been extruded through the laser-drilled filter medium or the particles may consist of polyisobutylene which has similarly been forced through the fine laser filter holes. The smallest particles present are extremely fine and are barely resolved at the present magnification. Consequently, the smallest class of particles cannot be clearly distinguished from the polymer matrix background.

An in-line image of the stretch wrap material, Figure 28, appears similar to the off-line image presented in Figure 27, discounting the presence of the image guide structure. The off-line image, however, is better focused and the particles are more clearly resolved than in the in-line image.

Thus the particles area distribution alone does not adequately quantify the contamination level present in recycled PE. A measure of particle concentration, in units of [number of particles/ mm³] is required in order to quantify the particulate matter. Table 5-1 summarizes the particulate concentration in the recycled PE evaluated. Concentrations are based on the fact that the optical system has a depth of field of 0.67 mm; this in part determines the sampling volume. A sample calculation of particle concentration may be found in Appendix E.

The first three batches of recycled HDPE were filtered through a Dutch weave screen of various mesh sizes (110, 120 and 125). The particle concentration associated with this material is very high , ranging from 176 to 237 particles/ mm³. In contrast, the LDPE stretch wrap, D-LDPE, which had been filtered through a laser filter having hole openings of 100 μm, contained approximately 1/3 of the particulate concentration, 64 particles/ mm³, as compared to the recycled plastic which had been passed through a Dutch weave filter.

TABLE 5-1: Particulate Concentration in Recycled Polyethylene

PE batch	filter type	mesh	aperture (μm)	# of particles mm ³
A-HDPE	Dutch weave screen	110	140	183
B-HDPE		120	122	237
C-HDPE		125	120	176
D-LDPE	laser filter	-	100	64

A direct comparison between the Dutch weave screen packs and the laser filter is not possible based on the above experiments, owing to the difference in the source material. The screen filtered material consisted entirely of post consumer high density polyethylene. Whereas the laser filtered material was recycled low density polyethylene stretch wrap which is inherently a purer material.

5.2 ASSESSMENT OF MELT FILTRATION

5.2.1 TRANSIENT TESTING

Polymer melt filtration was assessed in-line for the first time, due to the creation of the in-line particulate vision monitor. In transient testing, the filter remained stationary in order to produce a cumulative build-up of contaminants on the filter element over a 6 hour period. Recycled high density polyethylene, A-HDPE, was passed through the extruder and the continuous screen changer, equipped with a 55 μm screen, at 2 different operating temperatures. Table 5-2 summarizes the effect that temperature had on particle removal.

At a system temperature of 180°C, the particle concentration in the extrudate at time

TABLE 5-2: Melt Filtration: Effect of Temperature on Particle Removal

Time (hr)	180°C, 20 rpm		220°C, 20 rpm	
	# of particles mm ³	% of original concentration	# of particles mm ³	% of original concentration
0	198	100%	227	100%
2	150	76%	229	101%
4	132	67%	162	72%
6	136	69%	176	78%

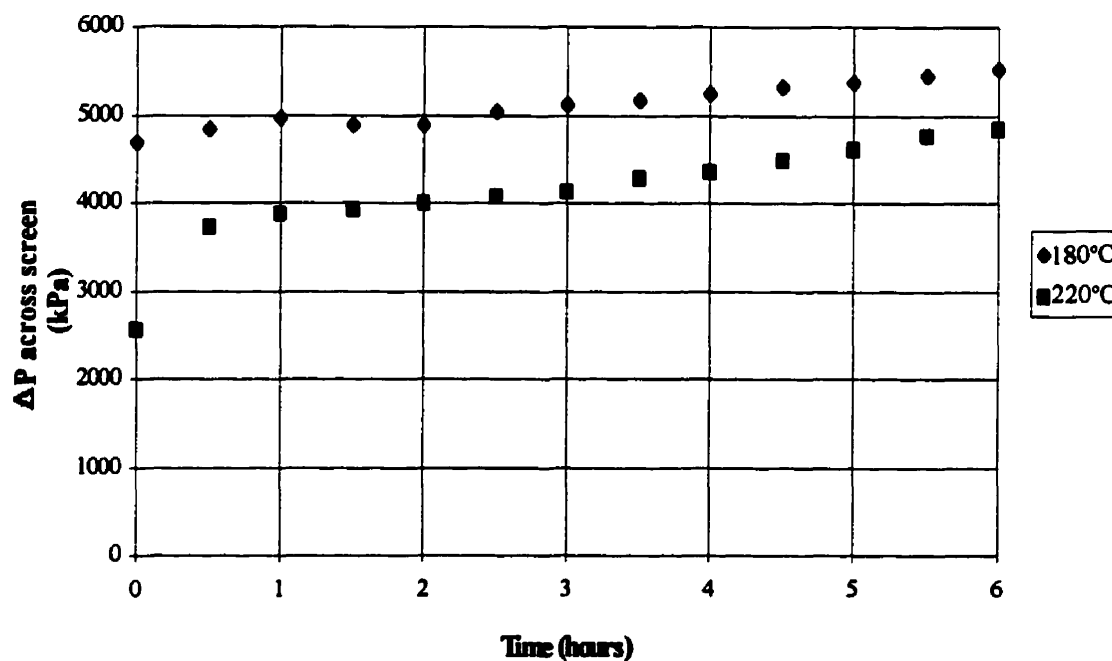


Figure 29: Pressure Difference Across Melt Filter versus Time
(55 μm screen, material= A-HDPE)

zero was 198 particles/ mm³. After 6 hours of melt filtration, the concentration was reduced to 136 particles/ mm³, or 69% of the original particle concentration. While at the elevated operating temperature of 220°C the particle concentration was initially 227 particles/ mm³ in the extrudate and only decreased to 176 particles/ mm³, or 78% of the original concentration, after 6 hours. The above results indicate that more particles are able to permeate the filter at higher temperatures.

Viscosity is inversely related to temperature. An increase in temperature will decrease the viscosity of the polymer and decrease the pressure drop across the filter. This decrease in resistance allows particles to travel through the filter medium more readily at elevated temperatures. There is increased particle blockage at the lower temperature, due to particle entrapment on the filter medium. Because of the increased resistance to flow sustained at the lower operating temperatures, it is more difficult for the particles to traverse the filter medium.

Figure 29 illustrates the relationship between the pressure difference across the filter screen as a function of both time and extrusion temperature. The pressure difference across the screen gradually increases with time as a filter cake develops on the screen surface and serves to increase the resistance to flow offered by the filter. Temperature affects the pressure drop by altering the viscosity of the polymer. Because pressure drop is directly proportional to viscosity, a decrease in polymer temperature will increase the pressure drop for the same flow rate. Conversely, an increase in temperature will decrease the pressure drop.

5.2.2 PULSE RESPONSE TESTING

A two-level factorial design was implemented to evaluate melt filtration through a pulse response technique involving glass beads. Glass beads were chosen as a tracer material because they are rigid bodies having a well defined size. The continuous screen changer was outfitted with a 75 μm screen. The extrusion system was operated at four different conditions which consisted of a combination of the following settings of temperature and screw speed: 180°C, 220°C, 20 rpm and 50 rpm.

5.2.2.1 GLASS BEAD SIZE DISTRIBUTION

The interaction plot in Figure 30 demonstrates the effect of temperature and screw speed on the exit glass bead distribution. The abscissa values indicate the screw speed of the extruder and the ordinate values are a measure of the filtered median glass bead diameter. At 220°C and 20 rpm, 50% of the glass beads emerging from the filter had a diameter of 41 μm or less. Whereas at the lower temperature of 180°C (and 20 rpm), 50% of the glass beads exiting the filter had a diameter of 67 μm or less.

From the interaction plot it can be concluded that an increase in temperature of the extrusion system results in an increase of fines in the filtrate. In addition, because the two lines on the interaction plot are parallel it can be deduced that there is no interaction effect between temperature and screw speed on the exit median glass bead diameter.

5.2.2.2 RESIDENCE TIME DISTRIBUTION

The in-line measurement of residence time distribution extends the applicability of the in-line particulate vision monitor to an important area of polymer extrusion. Through the

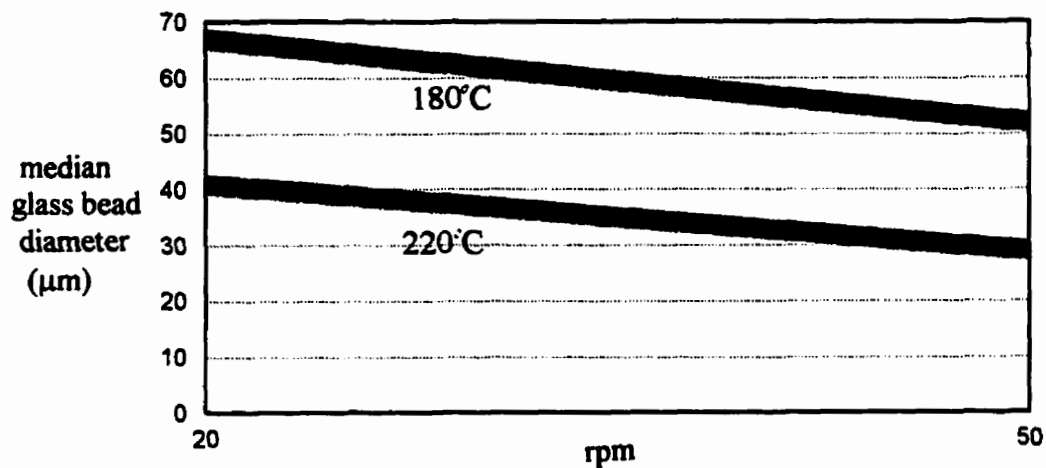


Figure 30: Interaction Plot: Effect of T and rpm on Glass Bead Distribution

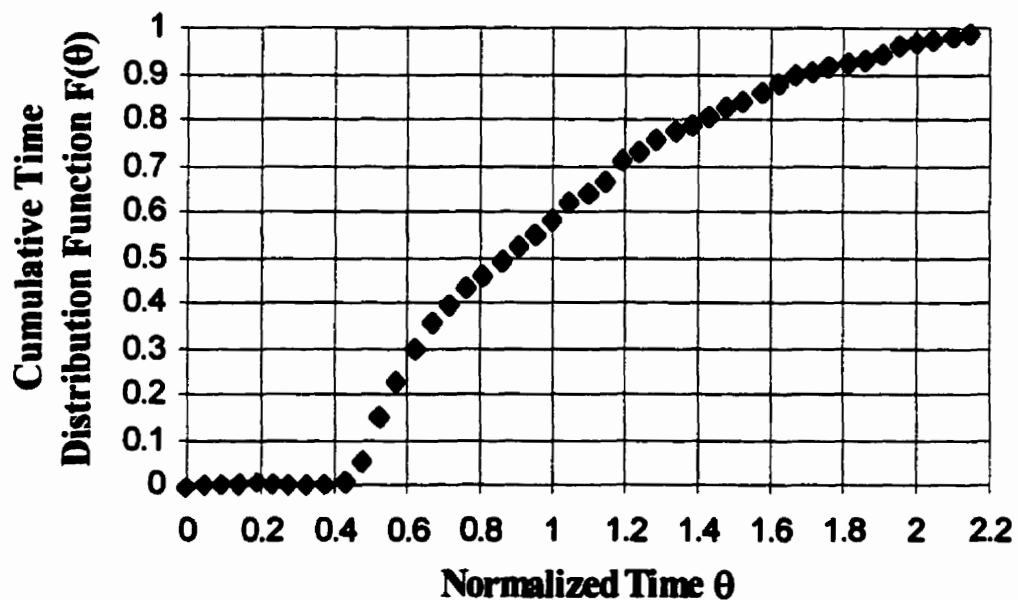


Figure 31: Cumulative Time Distribution in a Single Screw Extruder (180°C, 50 rpm, 75 μm screen)

pulse response testing conducted with the glass beads , the effect of the melt filter and two processing variables, temperature and screw speed, on the residence time distribution were studied.

A sample cumulative residence time distribution curve is shown in Figure 31 as a plot of Normalized Time θ versus the Cumulative Time Distribution Function $F(\theta)$. The extrusion conditions were 180°C, 50 rpm with a 75 μm screen for this particular plot.

Appendix F contains a sample residence time distribution function calculation.

A summary of the residence time distribution results for the 4 runs and the 2 controls (no screen present) are presented in Table 5-3. Overall, the mean residence time was inversely related to the screw speed. For example at 180°C and 20 rpm the mean residence time was 14.62 min while at 180°C and 50 rpm the mean residence time decreased to 6.99 min. The extrusion temperature had a negligible effect on the mean residence time.

TABLE 5-3: Summary of Residence Time Distributions

Run	Extrusion Conditions		mean residence time \bar{t} (min)	variance σ_t^2	dimensionless variance σ_θ^2	skewness factor As
	T (°C)	rpm				
1	180	20	14.62	13.62	0.064	152
2	180	50	6.99	9.85	0.20	53
3	220	20	14.61	16.37	0.077	206
4	220	50	7.65	10.28	0.18	37
control	(no screen)					
5	180	20	13.70	15.67	0.083	190
6	180	50	5.61	6.47	0.21	40

The presence of the screen, from the continuous melt filter, served to increase the mean residence time. The polymer had to travel an increased distance through the tortuous path of a Dutch weave stainless steel filter. At the lower screw speed, 20 rpm, the mean residence time increased an average of 0.92 min as compared to the control set up in which the screen was not present. At the elevated screw speed of 50 rpm, however, the mean residence time unexpectedly increased by an average of 1.71 min, compared to the control. The latter result contradicts the earlier finding in which the mean residence time was considered to be inversely related to the screw speed. An incorrect starting time for capturing the sample images of the tracer glass beads with the in-line particulate vision monitor would be the principal source of error to explain this discrepancy.

Values of the dimensionless variance are close to zero, indicating that the polymer flow pattern within the extrusion system tends towards plug flow with a small degree of back mixing. The lowest degree of back mixing, average value of $\sigma_0^2 = 0.071$, was present in the runs conducted at the lower screw speed setting of 20 rpm. Normally, with a general purpose mixing screw, a higher degree of back mixing would be expected.

The skewness factor, A_s , is used to differentiate between two distributions having similar values of mean and variance. Skewness refers to the asymmetry of a distribution and is equal to zero for a symmetric distribution. At 20 rpm the average skewness factor was 179 compared to the average skewness factor of 45 at 50 rpm.

The differential residence time distribution at the lower screw speed is more skewed to the right. This would manifest itself in a differential residence time distribution having a long thin tail pointed to the right with the bulk of the distribution concentrated in the left

most part of the plot. The long tail portion of a differential residence time distribution, (plot of Residence Time Distribution Function $E(\theta)$ versus Normalized Time θ), is due to material that has either been held in dead spaces within the extruder, retained by the screen or has adhered to the walls of the extruder. Although this represents a small part of the total mass, it requires a substantial amount of time to travel through the extruder and hence it has a relatively large impact on the mean residence time and the variance of the distribution.

6.0 CONCLUSIONS

- 1. An in-line particulate vision monitor was designed, constructed, and tested. The monitor, which operates in real-time with an extruder, yielded reproducible results in terms of particle area distributions, with a sample size of 10 images of recycled plastic waste, (about 1 000 particulate contaminants).**
- 2. The in-line particulate vision monitor provides information on both particle area distribution and particle concentration.**
- 3. An interpretation algorithm was developed using a median digital filter and the histogram minimum method to objectively analyze and quantify images through the image analysis software.**
- 4. Particulate contaminants observed in recycled polyethylene ranged in size from 30 to 25 000 μm^2 . Each batch possessed a bimodal particle area distribution, when evaluated at 200°C and 30 rpm. The 3 batches of unpigmented blow-moulding grade recycled HDPE had modes occurring at particle areas of 100 μm^2 and at 250 to 400 μm^2 . Whereas the laser filtered stretch wrap (LDPE) had greater values of particle area modes, with values of 400 and 1 000 μm^2 respectively.**
- 5. For the first time, melt filtration has been studied in-line, due to the creation of the in-line particulate vision monitor. Transient testing of melt filtration revealed that an**

increase in the extrusion temperature resulted in an increase in the number of particles passing through the filter. After operating for 6 hrs at 220°C and 20 rpm the particle concentration only decreased to 78% of the original concentration, compared to 69% at 180°C, with a 55µm Dutch twilled weave screen.

6. Pulse response testing of melt filtration conducted with glass beads through a two-level factorial design, resulted in an increase of fines in the filtrate at the higher operating temperature of 220°C. There was no interaction effect between temperature and screw speed on the exit median glass bead diameter.

7. Residence time information for an extrusion process was acquired in-line with the particulate vision monitor. The mean residence time in the extrusion system, (extruder, melt filter, die) was found to be 14.62 min at 20 rpm and 7.32 min at 40 rpm. The flow pattern within the extruder exhibited a low level of back mixing. Large values of the skewness factor, varying from 40 to 206, resulted from material that had either been retained by dead spaces inside the extruder, captured by the screen or became attached to the extruder wall.

7.0 RECOMMENDATIONS

- 1. Extend the interpretation algorithm for in-line images to enable quantitative identification of the various classes of contaminants present in recycled plastic waste. Shape descriptors could be used as a means of particle identification.**
- 2. A more efficient digital filtering step involving morphology filters, such as an open filter followed by a close filter, could be implemented in place of the current enhancement filter, the median filter, which can be time consuming.**
- 3. Illuminate the polymer stream in a more uniform fashion to facilitate the definition of particulate contaminants based on grey level threshold settings. Uniform illumination would result in the background polymer matrix possessing a relatively homogeneous grey level.**
- 4. Install a stroboscopic light source to freeze the motion of particulates in-line instead of stopping the polymer flow with a plug valve. A strobe light would be more practical when using the In-Line Particulate Vision Monitor on the industrial scale.**
- 5. Industrially, the in-line particulate vision monitor could be used as a detection mechanism to identify process upsets. By monitoring the changes in the particle area distribution as a function of time, a ruptured filter for example, could be detected.**
- 6. Monitoring quality is the precursor to controlling quality. The current ability to**

measure contaminants in-line could be integrated into a system that would be suitable for automatic process control of particulate contaminants in recycled plastic waste during extrusion.

8.0 REFERENCES

1. Boo, H.K., Mikofalvy, B.K., Summers, J.W., Mittendorf, D.H., and Sell, W.A., "Melt Filtration of Recycled PVC", *Antec*, 1934-1937, (1992).
2. Kilham, L.B., "A Systems Approach to Quality Control in the Production of Polymer Products", *Tappi J.*, 113-116, (1989).
3. Paul, M.H., "Fundamental Principles of the Filtration of non-Newtonian Liquids", in Filtration of Polymer Melts, pp. 1-28, Verein Deutscher Ingenieure, Germany, (1981).
4. Suetsugu, Y., Kikutani, T., Kyu, T., and White, J.L., "An Experimental Technique for Characterizing Dispersion in Compounds of Particulates in Thermoplastics using Small-Angle Light Scattering", *Colloid Polym. Sci.*, 118-131, February (1990).
5. Hansen, M.G., "A Review of On-Line Monitoring of Polymeric Processes by Infrared Spectrophotometry", *Antec*, 840-841, (1991).
6. Schirmer, R.E., and Gargus, A.G., "Monitoring Polymer Processing through Fiber Optics", *Am. Lab.*, 37-43, November (1988).
7. Kilham, L.B., and Riley, D.W., "Apparatus and Method for Polymer Melt Stream Analysis", *U.S. Patent* 4,529,306, July 16, 1985.
8. Kilham, L.B., "On-Line Particulate Analysis of Polymers and Compounds: in-the-melt vs. finished-product studies", *Converting and Packaging*, 156-159, March (1987).
9. Comeaux, L.K., and Chucta, J.D., "Analysis of the Flow Vision On-Line Gel Detector", *Antec*, 857-861, (1990).
10. Nir, M.M., "Implications of Post-Consumer Plastic Waste", *Plastics Eng.*, 46, 29-53, (1990).
11. Leaversuch, R.D., "Recycling Faces Reality as Bottom Line Looms", *Modern Plastics*, 71, 48-50, (1994).
12. Miller, S., "Cautions on the Use of Recycled Plastics", *Antec*, 2931-2936, (1993).
13. Hope, P.S., Parsons, D.A.G., Capaccio, G., and Kitchiner, M.J., "The Issue of Contamination in Recycling", *Makromol. Chem., Macromol. Symp.*, 57, 383-395, (1992).
14. Fleming, R.A., "Separation Technology of Used Polymers", *Makromol. Chem., Macromol. Symp.*, 57, 75-93, (1992).

15. Chien, D.C.H., and Penlidis, A., "On-Line Sensors for Polymerization Reactors", *Rev. Macromol. Chem. Phys.*, **30**, 1-42, (1990).
16. Mahlke, G., and Gössing, P., "Physics of Optical Waveguides", in Fiber Optic Cables, pp. 13-26, Siemens Aktiengesellschaft, Berlin, (1993).
17. Wolfbeis, O.S., "Fiber Optic Sensors", in Fiber Optic Chemical Sensors and Biosensors, pp. 4-8, CRC Press, Boston, (1991).
18. Miller, K.L., and Spatafore, R., "On-line Determination of Polyolefin Additives", *Antec*, 2524-2527, (1993).
19. Batra, J., Khettry, A., and Hansen, M.G., "In-Line Monitoring of Titanium Dioxide Content in Poly(Ethylene Terephthalate) Extrusion", *Polym. Eng. Sci.*, **34**, 1767-1772, (1994).
20. Hansen, M.G., and Khettry, A., "In-Line Monitoring of Molten Polymers: Near Infrared Spectroscopy, Robust Probes, and Rapid Data Analysis", *Polym. Eng. Sci.*, **34**, 1758-1766, (1994).
21. Hansen, M.G., Khettry, A., Batra, J., and Steward, D.A., "In-Line Near Infrared Monitoring of Polymeric Processes: Part II, Blends, Unfilled and Filled Polymers", *Antec*, 1437-1443, (1993).
22. Bur, A.J., Wang, F.W., Thomas, C.L., and Rose, J.L., "In-Line Optical Monitoring of Polymer Injection Molding", *Polym. Eng. Sci.*, **34**, 671-667, (1994).
23. Cielo, P., "Optical Sensors for On-Line Inspection of Industrial Material", *Opt. Eng.*, **32**, 2130-2137, (1993).
24. Naqwi, A.A., and Durst, F., "Analysis of Laser Light-Scattering Interferometric Devices for In-Line Diagnostics of Moving Particles", *Appl. Opt.*, **32**, 4003-4018, (1993).
25. Barth, H.G. and Sun, S., "Particle Size Analysis", *Anal. Chem.*, **65**, 55-66, (1993).
26. Yu, D., Esseghir, M., and Gogos, C.G., "The Use of "On-Line Optical Microscopy" for Monitoring Compounding and Other Polymer Processing Operations", *Antec*, 317-320, (1995).
27. Kilham, L.B., "On-Line Analyzers Boost Extrusion Productivity", *Modern Plastics*, 65-66, August, (1989).
28. Patel, H.N., and Lai, F.S., "Filtered Extrusion of Recycled Plastic Melt through

Constant Pressure Filtration System", *Antec*, 1192-1195, (1992).

29. Days, F., "Recycling is one factor raising the ceiling on performance technology", *Modern Plastics Encyclopedia*, E50-E51, November, (1994).
30. Carley, J.F., and Smith, W.C., "Design and Operation of Screen Packs", *Polym. Eng. Sci.*, **18**, 408-415, (1978).
31. Cassagnau, P., Mijangos, C., and Michel, A., "An Ultraviolet Method for the Determination of the Residence Time Distribution in a Twin Screw Extruder", *Poly. Eng. Sci.*, **31**, 772-778, (1991).
32. Wolf, D., Holin, N., and White, D.H., "Residence Time Distribution in a Commercial Twin-Screw Extruder", *Polym. Eng. Sci.*, **26**, 640-646, (1986).
33. Roark, R.J., and Young, W.C., "Flat Plates", in Formulas for Stresses and Strain, pp. 324-363, McGraw Hill, Toronto, (1985).
34. Desa, S., Cluett, W.R., Balke, S.T., and Horn, J.T., "Quality Monitoring of Recycled Plastic Waste During Extrusion: II. In-Line Particle Detection", *Antec*, 962-964, (1995).
35. Luk, J., "In-Line Observation of Polyethylene/Polystyrene Blend Morphology", B.A.Sc. thesis, *University of Toronto*, Toronto, (1995).
36. Desa, S., Reshadat, R., Cluett, W.R., Balke, S.T., and Horn, J.T., "In-Line Monitoring of Particulate Contaminants and Composition in Polymer Extrusion", *Polym. Mat. Sci. Eng. ACS*, **72**, 21-22, (1995).
37. Reshadat, R., Cluett, W.R., Balke, S.T., and Horn, J.T., "Quality Monitoring of Recycled Plastic Waste During Extrusion: I. In-Line Near Infrared Spectroscopy", *Antec*, 957-961, (1995).
38. Calidonio, F., "In-Line Colour Measurement of Pigmented Polyethylene During Extrusion", B.A.Sc. thesis, *University of Toronto*, Toronto, (1995).
39. Russ, J.C., "Discrimination and Thresholding", in Computer-Assisted Microscopy the Measurement and Analysis of Images, pp. 99-127, Plenum Press, New York, (1992).

APPENDIX A EQUIPMENT SPECIFICATIONS FOR ILLUMINATION, DETECTION AND IMAGE ANALYSIS SYSTEM

150W Illumination Source (Model 180, Dolan Jenner, Lawrence, MA)

lamp type : EKE

colour temperature: 3200 K

A variable intensity quartz halogen lamp; it peaks in the visible spectrum.

Quartz Light Guide (BXUV460, Dolan Jenner, Lawrence, MA)

element size: 0.10 mm

fibre bundle diameter: 6.4 mm

spectral transmittance: 0.20-2.1 microns

length: 1.5 m

Light guides are used to convey light, from a light source, to an area requiring illumination.

13mm Objective Lens (17° Field of View) (IG-1630, Scott Fiber Optics, Southbridge, MA)

The objective lens, attached to the distal end of the image guide, focuses the image onto the active area of the image guide. The parameters of the lens determine the magnification of the image.

Image Guide (IG-154-72, Schott Fiber Optics, Southbridge, MA)

format: 4mm x 4mm

element size: 10 microns

resolution: 50 LP/mm

maximum T: 120°C

length: 1.8 m

Image guides are used to transmit an image from one location to another. The image guide divides an image into 10 micron elements; it then transmits each part separately within the individual fibres and recombines them at the output end.

Relay lens (IG-1643, Schott Fiber Optics, Southbridge, MA)

The relay lens, (25mm, 1:1.4), magnifies the image two times and provides the link between the image guide and CCD video camera.

Sony Model XC NTSC format camera (Schott Fiber Optics, Southbridge, MA)

pick up device: interline transfer 1/2 inch CCD

picture elements: 768(H) x 494(V)

sensing area: 6.4mm x 4.8mm

signal system: NTSC standard

scanning system: 525 lines, 2:1 interlace, 30 frames /s

This is a CCD colour video camera. The Charged Coupled Device (CCD) is a

semi-conductor imaging sensor. It transforms the image (light) into a standard analogue video signal which can then be transferred to an analogue-to-digital converter in order to process the image information digitally.

Frame Grabber (DT-3851-8, Data Translation, Marlboro, MA)

Installed in the computer, the frame grabber, (an analogue to digital converter), allows the image analysis software to acquire and process images from video-output sources.

Global Lab Image 2.0 (Data Translation, Marlboro, MA)

An image analysis software package that will enhance, measure and classify features of interest in an image.

APPENDIX B
HISTOGRAMS OF RECYCLED POLYETHYLENE AND BLANK
IMAGE GUIDE

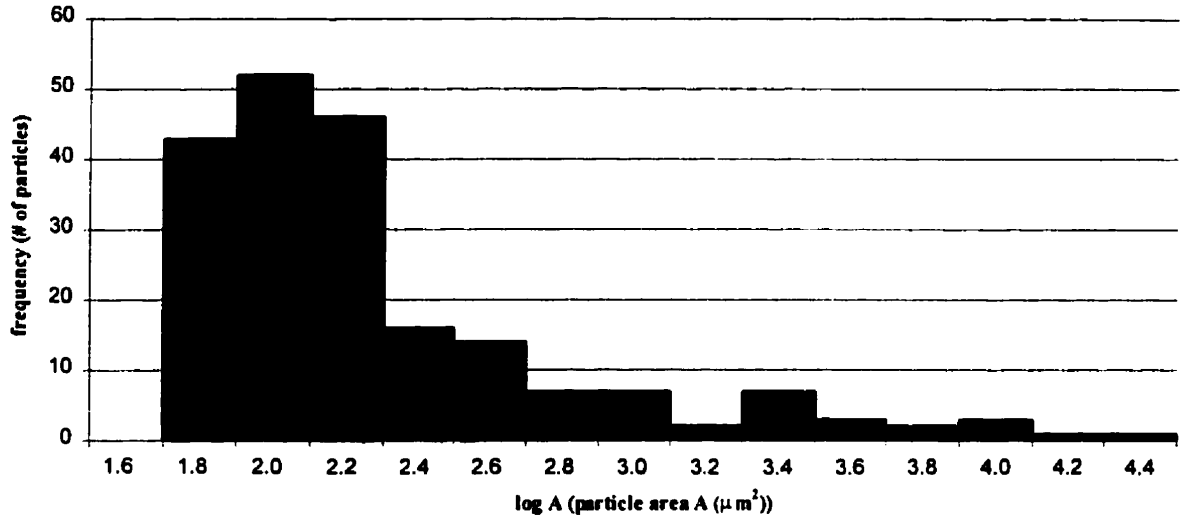


Figure B1: Image Histogram of Recycled Polyethylene (A-HDPE), 1 image
 (Recycled Polyethylene + Blank Image Guide)

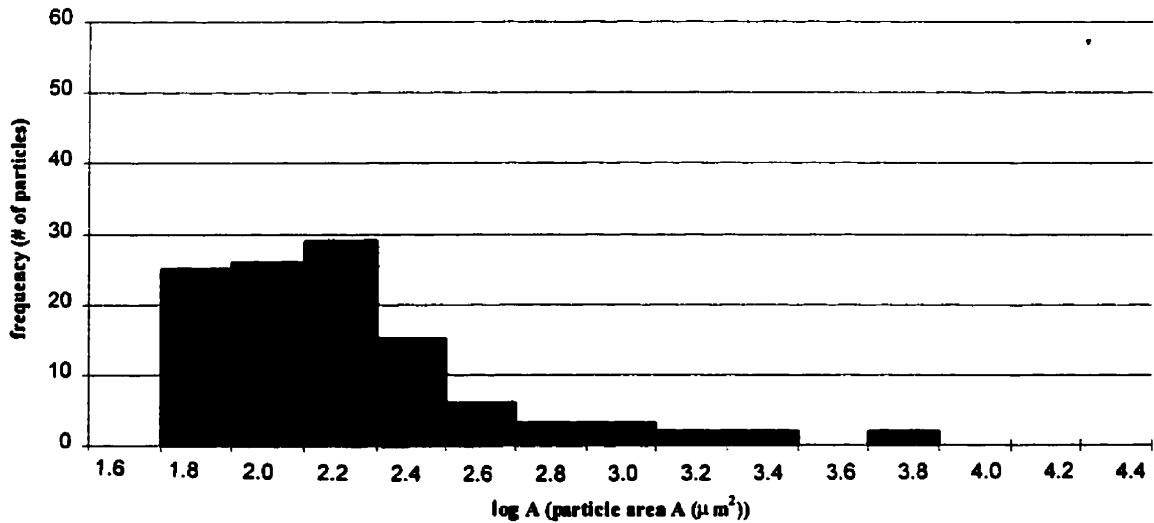


Figure B2: Histogram of Blank Image Guide

APPENDIX C

PARTICLE AREA DISTRIBUTION: SAMPLE CALCULATION

PE batch: A-HDPE, extruded at 200°C and 30 rpm

10 images

x	10 ^x	log IMAGE HISTOGRAM		BLANK HISTOGRAM		Fblank =F*(10 images)
		Bin (μm ²) (particle area)	Frequency (# of particles)	Bin (μm ²) (particle area)	Frequency (# of particles)	
1.5	31.6228	31.6227766	0	31.6227766	0	0
1.7	50.1187	50.11872336	0	50.11872336	0	0
1.9	79.4328	79.43282347	409	79.43282347	25	250
2.1	125.893	125.8925412	528	125.8925412	26	260
2.3	199.526	199.5262315	379	199.5262315	29	290
2.5	316.228	316.227766	288	316.227766	15	150
2.7	501.187	501.1872336	171	501.1872336	6	60
2.9	794.328	794.3282347	107	794.3282347	3	30
3.1	1258.93	1258.925412	67	1258.925412	3	30
3.3	1995.26	1995.262315	48	1995.262315	2	20
3.5	3162.28	3162.27766	34	3162.27766	2	20
3.7	5011.87	5011.872336	24	5011.872336	0	0
3.9	7943.28	7943.282347	14	7943.282347	1	10
4.1	12589.3	12589.25412	15	12589.25412	0	0
4.3	19952.6	19952.62315	12	19952.62315	0	0
4.5	31622.8	31622.7766	6	31622.7766	0	0
			10 images		1 image	10 images

actual frequency Fimage-Fblank	d(logA)	log(avg A)	%in range N(log A)	% per log(area) N(logA)/d(logA)
0				
0	0.2	1.6	0	0
159	0.2	1.8	16.19144603	80.95723014
268	0.2	2	27.29124236	136.4562118
89	0.2	2.2	9.063136456	45.31568228
138	0.2	2.4	14.05295316	70.26476578
111	0.2	2.6	11.30346232	56.51731161
77	0.2	2.8	7.84114053	39.20570265
37	0.2	3	3.767820774	18.83910387
28	0.2	3.2	2.851323829	14.25661914
14	0.2	3.4	1.425661914	7.128309572
24	0.2	3.6	2.443991853	12.21995927
4	0.2	3.8	0.407331976	2.036659878
15	0.2	4	1.527494908	7.637474542
12	0.2	4.2	1.221995927	6.109979633
6	0.2	4.4	0.610997963	3.054989817
total= 982			total= 100%	
# of particles in 10 images				

APPENDIX D
IN-LINE AND OFF-LINE IMAGES OF RECYCLED HIGH DENSITY
POLYETHYLENE

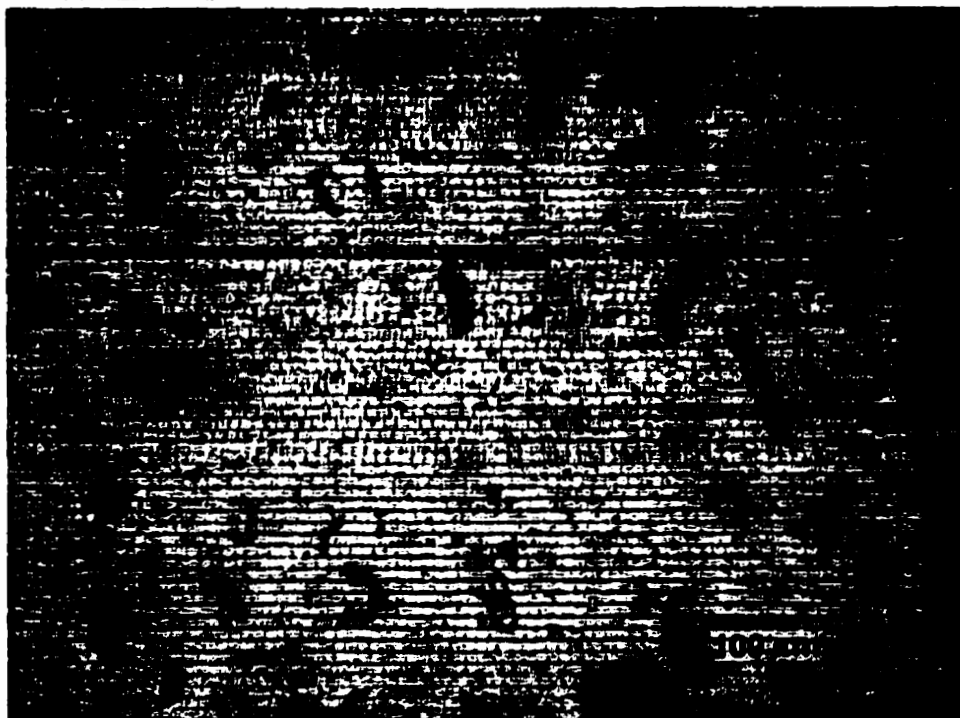


Figure D1: In-Line Image of A-HDPE During Extrusion (200°C, 30 rpm)

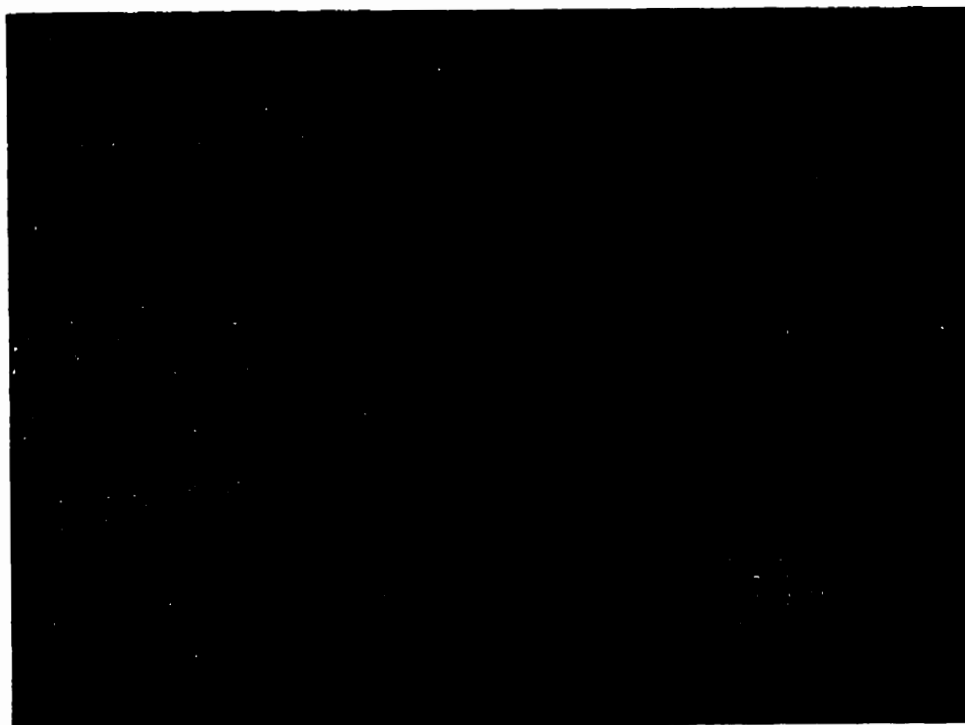


Figure D2: Off-Line Image of A-HDPE (200°C, transmission illumination)



Figure D3: In-Line Image of B-HDPE During Extrusion (200°C, 30 rpm)

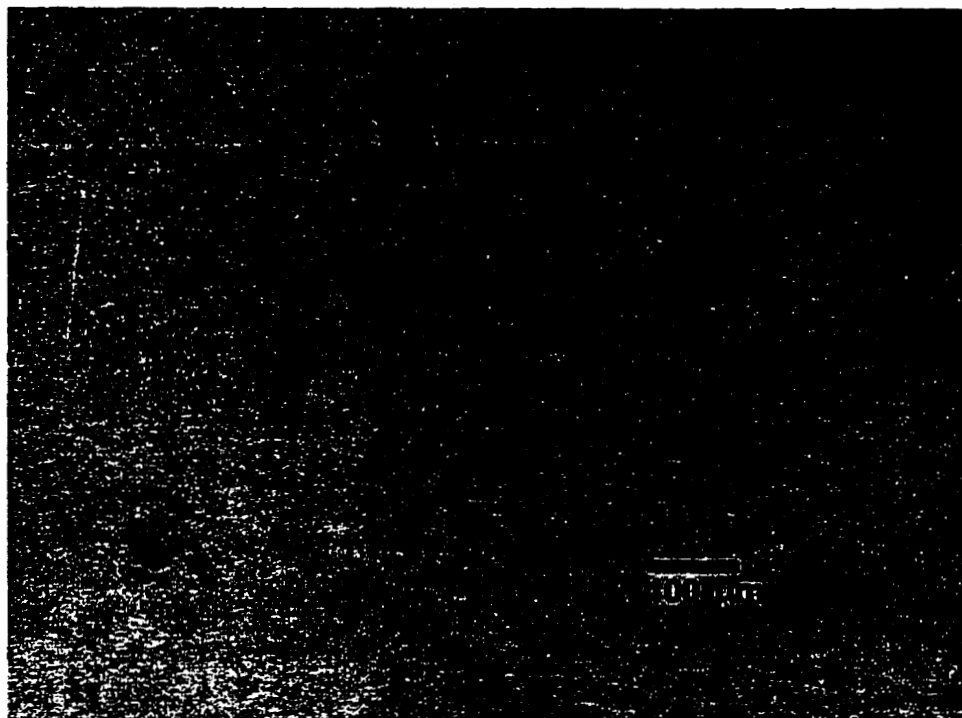


Figure D4: Off-Line Image of B-HDPE (200°C, transmission illumination)



Figure D5: In-Line Image of C-HDPE During Extrusion (200°C, 30 rpm)



Figure D6: Off-Line Image of C-HDPE (200°C, transmission illumination)

APPENDIX E

PARTICLE CONCENTRATION: SAMPLE CALCULATION

PE batch: A-HDPE, extruded at 200°C and 30 rpm
10 images

10 images contain a total of 982 particles (see "actual frequency" column in APPENDIX C)

Volume of monitored section of polymer stream
= (image length)(image width)(depth of field of image)(# of images)
= (1.025 mm)(0.783 mm)(0.67 mm)(10 images)
= 5.377 mm³

Particle concentration
=(# of particles)/ (Volume of monitored section)
= 982 particles/ 5.377 mm³
= 183 particles /mm³

APPENDIX F

RESIDENCE TIME DISTRIBUTION: SAMPLE CALCULATION

-PE batch: A-HDPE

-5 g pulse of glass beads

- extrusion conditions: 180°C, 50 rpm

-continuous screen changer: 200 mesh, (75 μ m aperture)

t_m = 6.9903 min (mean residence time)

Δt = 0.3333 min

$\Delta \theta$ = 0.0472

σ^2 = 9.8535 (variance)

s^2_e = 0.2017 (dimensionless variance)

A_s = 52.6366 (skewness of distribution)

time (min)	# of glass beads						variance	skewness		
t	C(t)	C(t)·t	$\theta=t/t_m$	C(t)· Δt	E(t)	$E(\theta)=t_m \cdot E(t)$	σ^2	A_s	$E(\theta) \cdot \Delta \theta$	F(θ)
3	2	6	0.4292	0.6667	0.0289	0.2026	0.1538	-1.3670	0.00957	0.00957
3.33	9	29.97	0.4764	3	0.1304	0.9118	0.5825	-4.7481	0.0430	0.05261
3.67	20	73.4	0.5250	6.6667	0.2899	2.0262	1.0652	-7.8757	0.09565	0.14826
4	16	64	0.5722	5.3333	0.2319	1.6209	0.6912	-4.6025	0.07652	0.22478
4.33	15	64.95	0.6194	5	0.2174	1.5196	0.5128	-3.0381	0.07174	0.29652
4.67	12	56.04	0.6681	4	0.1739	1.2157	0.3121	-1.6126	0.05739	0.35391
5	8	40	0.7153	2.6667	0.1159	0.8105	0.1531	-0.6785	0.03826	0.39217
5.33	8	42.64	0.7625	2.6667	0.1159	0.8105	0.1065	-0.3939	0.03826	0.43043
5.67	6	34.02	0.8111	2	0.0870	0.6079	0.0505	-0.1486	0.02870	0.45913
6	6	36	0.8583	2	0.0870	0.6079	0.0284	-0.0627	0.02870	0.48783
6.33	7	44.31	0.9055	2.3333	0.1014	0.7092	0.0147	-0.0217	0.03348	0.5213
6.67	6	40.02	0.9542	2	0.0870	0.6079	0.0030	-0.0021	0.02870	0.55
7	6	42	1.0014	2	0.0870	0.6079	2.73E-06	0.0000	0.02870	0.5787
7.33	8	58.64	1.0486	2.6667	0.1159	0.8105	0.0045	0.0034	0.03826	0.61696
7.67	5	38.35	1.0972	1.6667	0.0725	0.5065	0.0112	0.0169	0.02391	0.64087
8	5	40	1.1444	1.6667	0.0725	0.5065	0.0246	0.0554	0.02391	0.66478
8.33	9	74.97	1.1917	3	0.1304	0.9118	0.0780	0.2328	0.0430	0.70783
8.67	5	43.35	1.2403	1.6667	0.0725	0.5065	0.0682	0.2549	0.02391	0.73174
9	5	45	1.2875	1.6667	0.0725	0.5065	0.0976	0.4366	0.02391	0.75565
9.33	4	37.32	1.3347	1.3333	0.0580	0.4052	0.1058	0.5512	0.01913	0.77478
9.67	3	29.01	1.3833	1	0.0435	0.3039	0.1041	0.6210	0.01435	0.78913
10	3	30	1.4306	1	0.0435	0.3039	0.1313	0.8799	0.01435	0.80348
10.33	4	41.32	1.4778	1.3333	0.0580	0.4052	0.2155	1.6029	0.01913	0.82261
10.67	4	42.68	1.5264	1.3333	0.0580	0.4052	0.2616	2.1440	0.01913	0.84174
11	4	44	1.5736	1.3333	0.0580	0.4052	0.3107	2.7741	0.01913	0.86087
11.33	3	33.99	1.6208	1	0.0435	0.3039	0.2729	2.6377	0.01435	0.87522
11.67	4	46.68	1.6695	1.3333	0.0580	0.4052	0.4232	4.4101	0.01913	0.89435
12	2	24	1.7167	0.6667	0.0290	0.2026	0.2425	2.7052	0.00957	0.90391
12.33	3	36.99	1.7639	1	0.0435	0.3039	0.4132	4.9137	0.01435	0.91826
12.67	1	12.67	1.8125	0.3333	0.0145	0.1013	0.1558	1.9711	0.00478	0.92304
13	1	13	1.8597	0.3333	0.0145	0.1013	0.1745	2.3350	0.00478	0.92783
13.33	3	39.99	1.9069	1	0.0435	0.3039	0.5825	8.2236	0.01435	0.94217
13.67	4	54.68	1.9556	1.3333	0.0580	0.4052	0.8622	12.8252	0.01913	0.9613
14	2	28	2.0028	0.6667	0.0290	0.2026	0.4747	7.4107	0.00957	0.97087
14.33	1	14.33	2.0500	0.3333	0.0145	0.1013	0.2902	4.2537	0.00478	0.97565
14.67	1	14.67	2.0986	0.3333	0.0145	0.1013	0.2849	4.8726	0.00478	0.98043
15	2	30	2.1458	0.6667	0.0290	0.2026	0.8199	11.0563	0.00957	0.99
	207	1446.99		68.9999			9.8535	52.6366		